

**CORNEA ENGINEERING  
ON  
BIODEGRADABLE POLYESTERS**

**A THESIS SUBMITTED TO  
THE GRADUATE SCHOOL OF NATURAL AND APPLIED SCIENCES  
OF  
MIDDLE EAST TECHNICAL UNIVERSITY**

**BY**

**PINAR ZORLUTUNA**

**IN PARTIAL FULFILLMENT OF THE REQUIREMENTS  
FOR  
THE DEGREE OF MASTER OF SCIENCE  
IN  
BIOTECHNOLOGY**

**JANUARY 2005**

Approval of the Graduate School of Natural and Applied Sciences

\_\_\_\_\_  
Prof. Dr. Canan Özgen  
Director

I certify that this thesis satisfies all the requirements as a thesis for the degree of Master of Science.

\_\_\_\_\_  
Assoc. Prof. Dr. Dilek Sanin  
Head of Department

This is to certify that we have read this thesis and that in our opinion it is fully adequate, in scope and quality, as a thesis for the degree of Master of Science in Biotechnology.

\_\_\_\_\_  
Asst. Prof. Dr. Ayşen Tezcaner  
Co-Supervisor

\_\_\_\_\_  
Prof. Dr. Vasıf Hasırcı  
Supervisor

**Examining Committee Members**

|                          |                     |       |
|--------------------------|---------------------|-------|
| Prof. Dr. İnci Togan     | (METU,BIO)          | _____ |
| Prof. Dr. Vasıf Hasırcı  | (METU,BIO)          | _____ |
| Prof. Dr. Atilla Aydınlı | (Bilkent Uni.,PHYS) | _____ |
| Prof. Dr. Gülay Özcengiz | (METU,BIO)          | _____ |
| Prof. Dr. Mesude İşcan   | (METU,BIO)          | _____ |

**I hereby declare that all information in this document has been obtained and presented in accordance with academic rules and ethical conduct. I also declare that, as required by these rules and conduct, I have fully cited and referenced all material and results that are not original to this work.**

Name, Last name :

Signature :

## **ABSTRACT**

# **CORNEA ENGINEERING ON BIODEGRADABLE POLYESTERS**

Zorlutuna, Pınar

M. Sc., Department of Biotechnology

Supervisor: Prof. Vasıf Hasırcı

Co-Supervisor: Asst. Prof. Ayşen Tezcaner

January 2005, 66 pages

Cornea is the outermost layer of the eye and has an important role in vision. Damage of cornea due to injuries or infections could lead to blindness lowering the quality of life of the patient severely. In such cases, transplantation or artificial corneas have been used for treatment but both had drawbacks. The novel approach for corneal replacements is the tissue engineering of the cornea, a promising method which would be free of these drawbacks, if successful.

In this study, carriers for tissue engineering of the cornea were designed and tested in vitro. Blends of biodegradable and biocompatible polyesters of natural (PHBV8) and synthetic (PLLA) origin were used to construct these carriers. For the epithelial layer of the cornea, PLLA-PHBV8 micropatterned films were prepared with solvent casting and seeded with D407 (retinal pigment epithelial) cells. In order to achieve proper cell growth, the films were coated with fibronectin. For the stromal layer of the cornea, highly porous foams of PLLA-PHBV8 were prepared by lyophilization and seeded with 3T3 cells (fibroblasts). A new approach was developed to create a combination of the film and the foam to obtain a surface patterned, 3 dimensional cell carrier. These carriers were seeded with Saos-2 cells (osteosarcoma cells) in the preliminary optimization studies and with D407 and 3T3 cells in further studies. The cell numbers on the carriers were quantified by using MTS assay (non-radioactive cell proliferation assay) and the cell proliferation on polymeric carriers was significantly higher than that of control (Tissue culture polystyrene) by the day 14. Characterization of these cells and the carrier was done using a variety of microscopic methods. The micrographs showed that the foam had a highly porous structure and the pores were interconnected. 3T3 cells were found to be distributed quite homogeneously at the seeding site, but due to the high thickness of the foam, the cells could not sufficiently populate the core (central parts of the foam) during the given incubation time. The micropatterned film allowed multilayer formation of D407 cells. The functionality of the cells seeded on the carriers was examined by immunohistochemistry. These analyses proved that the cells retained their phenotype during culturing. D407 cells formed tight junctions characteristic of epithelial cells, and 3T3 cells deposited collagen type I into the foams. Based on the results, it can be concluded that the 3-D PLLA-PHBV8 construct with surface patterns have a serious potential for use as a tissue engineering carrier for the reconstruction of the cornea.

**Key words:** Tissue engineering, cornea, polymeric carrier, biodegradable, polyester.

## ÖZ

### **BİYOBOZUNUR POLYESTERLERDE KORNEA DOKU MÜHENDİSLİĞİ**

Zorlutuna, Pınar

Yüksek Lisans, Biyoteknoloji Bölümü

Tez Yöneticisi: Prof. Dr. Vasıf Hasırcı

Ortak Tez Yöneticisi: Yrd. Doç. Dr. Ayşen Tezcaner

Ocak 2005, 66 sayfa

Kornea, görme işlevinde önemli bir rol alan, gözün en dış tabakasıdır. Korneanın yaralanma veya enfeksiyon sonucunda hasar görmesi körlüğe yol açar ki, bu da hastanın yaşam kalitesini önemli ölçüde düşürür. Böyle durumlarda transplantasyon ya da yapay kornealar tedavi için günümüzde en yaygın olarak uygulanan yaklaşımlardır. Ancak her iki yöntemin de olumsuz yanları vardır. Korneanın doku mühendisliği yoluyla üretimi başarılı olduğu takdirde, bu olumsuzluklardan arınmış daha etkili bir tedavi yöntemi geliştirilmiş olacaktır.

Bu arařtırmada, kornea doku mhendislięinde kullanılmak zere hcre tařıyıcıları tasarlanmış ve in vitro olarak test edilmiřtir. Bu hcre tařıyıcıları doęal (PHBV8) ve sentetik kaynaklı (PLLA), biyobozunur ve biyouyumlu polyesterlerin karıřımları kullanılarak hazırlanmıřtır. Korneanın epitel tabakası iin, PLLA-PHBV8 mikrodeseenli filmler dkme yntemi ile hazırlanmıř ve zerlerine D407 (Retinal pigment epitel) hcreleri ekilmiřtir. Stroma tabakası iin ise, ok gzenekli kpkler liyofilizasyon yntemi ile hazırlanmıř ve bunların ierisine 3T3 (fibroblastik hcre) hcreleri ekilmiřtir. Yeni bir metod geliřtirilerek film ve kpk birleřtirilmiř, yzeyi mikrodeseenli 3 boyutlu bir tařıyıcı elde edilmiř ve bu tařıyıcıların n alıřmalarında Saos-2 hcreleri (osteasarkoma hcreleri) kullanılmıřtır. Sonraki alıřmalarda, D407 ve 3T3 hcreleri ekilmiřtir. Hcre miktarı MTS testi (radyoaktif olmayan hcre oęalımı tayin testi) kullanılarak belirlenmiř ve 14. gnn sonunda, polimerik tařıyıcıların zerine ekilen hcrelerin kontrole (polistiren doku kltr kabı) kıyasla daha fazla oęaldıęı gzlenmiřtir. Bu hcrelerin ve tařıyıcıların karakterizasyonu iin bir ok mikroskopi teknikleri kullanılmıřtır. Elde edilen mikrograflardan polimerik kpęn ok gzenekli bir yapıya sahip olduęu ve bu gzeneklerin birbirlerine baęlı oldukları anlařılmıřtır. Bu yapı, ekim blgesindeki 3T3 hcrelerinin olduka homojen bir řekilde daęılmasına olanak saęlamıřtır. Fakat, kpk kalınlıęının fazlalıęı sebebi ile hcreler uygulanan inkbasyon sresi ierisinde kpęn en i blgelerine kadar ulařamamıřlardır. Mikrodeseenli film, D407 hcrelerinin ok katmanlı bir yapı oluřturmalarına olanak saęlamıřtır. Tařıyıcılara ekilmiř hcrelerin iřlevsellikleri immnhistokimyasal yntemler kullanılarak incelenmiřtir. Bu analizler hcrelerin fenotiplerini kltr sresince koruduklarını gstermiřtir. D407 hcreleri epitel hcrelerin karakteristik zellięi olan sıkı baęlantıları (tight junction) kurmuř ve 3T3 hcreleri kpęn ierisine tip I kollajen salgılamıřtır. Sonu olarak, PLLA-PHBV8 mikrodeseenli yzeyli ve yksek gzenekli tařıyıcıların korneanın doku mhendislięi yntemiyle oluřturulmasına uygun olduęu kanısına varılmıřtır.

**Anahtar kelimeler:** Doku mhendislięi, kornea, polimerik tařıyıcı, biyobozunur, polyester.

*Dedicated to the memory of  
Prof. Dr. Raci Bademli*

## ACKNOWLEDGEMENT

I would like to express my most sincere gratitude to Prof. Vasıf HASIRCI and Assist. Prof. Ayşen TEZCANER for their valuable advice, guidance and continuous encouragement and support throughout this study.

I wish to extend my thanks to Prof. Atilla AYDINLI and İsa KIYAT (both of Bilkent University) for providing the micropatterned templates, an indispensable component of this study.

I am grateful to Assist. Prof. Dilek KESKİN and Assist. Prof. Gamze TORUN KÖSE for their valuable advice and support during this study.

I would like to thank to my lab partner Engin VRANA for his friendship and support during the long hours we spent working hard together to achieve a common goal.

I wish to thank to all my friends Halime KENAR, Şerife AYAZ, Deniz YÜCEL, Oya TAĞIT, Süleyman COŞKUN, Buket BAŞMANAV, Erkin AYDIN and our technician Zeynel AKIN for their support in this study, and to our staff Hakan ŞEN for his continuous help.

Finally, I would like to express my deepest gratitude to my family, for their understanding, patience and continuous support and trust in me, without which it would not be possible to succeed.

This project was conducted as a part of the EU FP6 STREP Project “Cornea Engineering”. I am grateful for their support that was essential for the accomplishment of this research.

## TABLE OF CONTENTS

|   |      |
|---|------|
| <b>ABSTRACT</b> .....   | iv   |
| <b>ÖZ</b> .....   | vi   |
| <b>DEDICATION</b> .....   | viii |
| <b>ACNOWLEDGEMENTS</b> .....                                    | ix   |
| <b>TABLE OF CONTENTS</b> .....                                  | x    |
| <b>LIST OF TABLES</b> .....                                     | xiv  |
| <b>LIST OF FIGURES</b> .....                                    | xv   |
| <b>LIST OF ABBREVIATIONS</b> .....                              | xvii |
| <b>CHAPTER</b> .....  |      |
| <b>1. INTRODUCTION</b> .....                                    | 1    |
| 1.1. Tissue engineering.....                                    | 1    |
| 1.1.1. Components in Tissue Engineering.....                    | 1    |
| 1.1.1.1. Carriers.....  | 1    |
| 1.1.1.1.1. Natural Origin.....                                  | 3    |
| 1.1.1.1.1.1. Collagen.....                                      | 3    |
| 1.1.1.1.1.2. Polyhydroxyalkanoates (PHA).....                   | 3    |
| 1.1.1.1.2. Synthetic Origin.....                                | 3    |
| 1.1.1.2. Cell.....  | 4    |
| 1.2. Cornea Engineering.....                                    | 5    |
| 1.2.1. Function and Structure of the Cornea.....                | 5    |
| 1.2.2. Diseases and Disorders Affecting the Cornea.....         | 9    |
| 1.2.3. Corneal Response to Injury.....                          | 9    |
| 1.2.4. Approaches for the Repair of Severe Corneal Damages..... | 10   |
| 1.2.4.1. Corneal Transplantation.....                           | 10   |
| 1.2.4.2. Keratoprotheses.....                                   | 11   |
| 1.2.4.3. Tissue Engineering.....                                | 12   |

|  |    |
|--|----|
| <b>2. MATERIALS AND METHODS</b> .....  | 15 |
| 2.1. Materials.....  | 15 |
| 2.2. Methods.....  | 16 |
| 2.2.1. Preparation of Carriers.....  | 16 |
| 2.2.1.1. Preparation of Micropatterned Films.....                                    | 16 |
| 2.2.1.2. Preparation of Foams.....   | 17 |
| 2.2.1.3. Preparation of Three Dimensional (3-D) Micropatterned<br>Cell Carriers..... | 17 |
| 2.2.2. Characterization of Carriers.....   | 18 |
| 2.2.2.1. Physical Characterization.....  | 18 |
| 2.2.2.2. Microscopic Characterization.....   | 19 |
| 2.2.3. Cell Culture Studies.....   | 19 |
| 2.2.3.1. Saos-2 Cells.....   | 19 |
| 2.2.3.2. D407 (Retinal Pigment Epithelial Cell Line) and 3T3 cells                   | 20 |
| 2.2.3.2.1. Cell Culture.....   | 20 |
| 2.2.3.2.2. Cell Seeding onto Carriers.....   | 20 |
| 2.2.3.2.2.1. Micropatterned Films.....   | 20 |
| 2.2.3.2.2.2. Foams.....  | 21 |
| 2.2.3.2.2.3. 3-D Constructs.....   | 21 |
| 2.2.3.2.3. Characterization of Cell Seeded Carriers.....                             | 22 |
| 2.2.3.2.3.1. D407 Cells.....   | 22 |
| 2.2.3.2.3.1.1. Cell Proliferation.....   | 22 |
| 2.2.3.2.3.1.2. Morphology of Cells.....  | 23 |
| 2.2.3.2.3.1.3. Immunohistochemical Studies.....                                      | 23 |
| 2.2.3.2.3.2. 3T3 Cells.....  | 24 |
| 2.2.3.2.3.2.1. Cell Proliferation.....   | 24 |
| 2.2.3.2.3.2.2. Morphology of Cells.....  | 24 |
| 2.2.3.2.3.2.3. Immunohistochemical Studies.....                                      | 25 |

|  |    |
|--|----|
| <b>3. RESULTS AND DISCUSSION</b> .....                                 | 26 |
| 3.1. Physical and Microscopic Characterization of Films and Foams..... | 26 |
| 3.1.1. Foam Density.....   | 26 |
| 3.1.2. Foam and Film Thickness.....                                    | 26 |
| 3.1.3. Microscopy Observations.....                                    | 27 |
| 3.1.3.1. SEM.....  | 27 |
| 3.1.3.2. Light Microscopy.....   | 28 |
| 3.2. In Vitro Studies.....   | 28 |
| 3.2.1. Saos-2 Cells on 3-D Construct.....                              | 29 |
| 3.2.2. D407 Cells on Patterned Films.....                              | 30 |
| 3.2.2.1. Without Fibronectin.....                                      | 30 |
| 3.2.2.1.1. Cell Proliferation.....                                     | 30 |
| 3.2.2.1.2. Microscopy Observations.....                                | 31 |
| 3.2.2.2. With Fibronectin.....   | 33 |
| 3.2.2.2.1. Cell Proliferation.....                                     | 33 |
| 3.2.2.2.2. Microscopy Observations.....                                | 34 |
| 3.2.2.2.3. Immunohistochemical Analysis.....                           | 37 |
| 3.2.2.2.3.1. Anti Pan-Cytokeratin Staining.....                        | 37 |
| 3.2.2.2.3.2. Anti ZO-1 Staining.....                                   | 38 |
| 3.2.3. 3T3 Cells on Foams.....   | 40 |
| 3.2.3.1. Cell Proliferation.....                                       | 40 |
| 3.2.3.2. Microscopy Observations.....                                  | 43 |
| 3.2.3.2.1. SEM.....  | 43 |
| 3.2.3.2.2. Confocal Microscopy.....                                    | 45 |
| 3.2.4. D407 and 3T3 Cells on the 3-D Construct.....                    | 46 |
| 3.2.4.1. Cell Proliferation .....                                      | 46 |
| 3.2.4.2. Microscopy Observations.....                                  | 47 |
| 3.2.4.2.1. Fluorescence Microscopy.....                                | 47 |
| 3.2.4.2.2. SEM.....  | 49 |

|   |           |
|---|-----------|
| 3.2.4.3. Immunohistochemical Analysis.....    | 52        |
| 3.2.4.3.1. Anti Collagen Type-1 Staining..... | 52        |
| <b>4. CONCLUSION.....</b>                     | <b>54</b> |
| <b>REFERENCES.....</b>                        | <b>56</b> |
| <b>APPENDICES.....</b>                        |           |
| <b>A.....</b>                                 | <b>65</b> |
| <b>B.....</b>                                 | <b>66</b> |

## LIST OF TABLES

### TABLES

|  |    |
|--|----|
| 2.1. Dimensions and geometry of micropatterned templates.....  | 17 |
| 3.1. The average thickness of films, foams and film-foams..... | 27 |

## LIST OF FIGURES

### FIGURES

|  |    |
|--|----|
| 1.1. Structure of the eye.....   | 6  |
| 1.2. Orthogonal orientation of collagen fibers in the corneal stroma.....  | 7  |
| 1.3. Layers of the cornea.....   | 7  |
| 2.1. Cross-section of A3, C3 and D1 templates.....   | 16 |
| 3.1. The SEM micrographs of PLLA-PHBV8 cell carriers.....  | 27 |
| 3.2. Light microscopy of foams.....  | 28 |
| 3.3. SEM micrographs of Saos-2 cells on the 3-D construct.....   | 29 |
| 3.4. Growth profile of D407 cells on 3 different micropatterned PLLA-PHBV8 films and TCPS (control).....                 | 31 |
| 3.5. Fluorescence micrographs of D407 cells seeded on the A3, C3 and D1 patterned films.....                             | 32 |
| 3.6. Growth profile of D407 cells on micropatterned PLLA-PHBV8 film and TCPS (control).....                              | 34 |
| 3.7. D407 cells on films, stained with Acridine orange, on day 1.....  | 35 |
| 3.8. D407 cells on films, stained with Acridine orange, on day 4.....  | 35 |
| 3.9. D407 cells on films, stained with Acridine orange, on day 7.....  | 36 |
| 3.10. D407 cells on films, stained with Acridine orange, on day 10.....  | 36 |
| 3.11. D407 cells on films, stained with Acridine orange, on day 14.....  | 37 |
| 3.12. Anti Pan-Cytokeratin staining of D407 cells on films on days 1.....  | 38 |
| 3.13. Anti ZO-1 staining of D407 cells on the films on days 1.....   | 39 |
| 3.14. Growth profile of 3T3 cells ( initial seeding density of $5 \times 10^5$ cells) on foams and TCPS (control).....   | 41 |
| 3.15. Growth profile of 3T3 cells ( initial seeding density of $2.5 \times 10^5$ cells) on foams and TCPS (control)..... | 42 |

|   |    |
|---|----|
| <b>3.16.</b> Growth profile of 3T3 cells with different initial seeding densities (2.5x10 <sup>5</sup> and 5x10 <sup>5</sup> ) on PLLA-PHBV8 foams..... | 42 |
| <b>3.17.</b> SEM micrographs of 3T3 seeded PLLA-PHBV8 foams on day 7.....   | 44 |
| <b>3.18.</b> SEM micrographs of 3T3 seeded PLLA-PHBV8 foams on day 14.....  | 45 |
| <b>3.19.</b> Confocal microscopy of 3T3 seeded PLLA-PHBV8 foams at day 14.....  | 46 |
| <b>3.20.</b> Growth profile of D407 and 3T3 cells on 3-D construct and TCPS (control).....  | 47 |
| <b>3.21.</b> 3T3 of the 3-D construct (stained with Acridine orange, at day 7).....   | 48 |
| <b>3.22.</b> 3T3 and D407 cells on 3-D construct, stained with Acridine orange, on day 14.....  | 48 |
| <b>3.23.</b> SEM micrographs of 3-D construct on day 7.....   | 50 |
| <b>3.24.</b> SEM micrographs of 3-D construct at day 14.....  | 51 |
| <b>3.25.</b> Anti collagen type I staining of 3T3 cells on 3-D construct at day 7.....  | 52 |
| <b>3.26.</b> Anti collagen type I staining of 3T3 cells on 3-D construct at day 14.....   | 52 |
| <b>3.27.</b> Comparison of unseeded and seeded, therefore, collagen deposited foam.....   | 52 |
| <b>A.1.</b> D407 calibration curve obtained by MTS assay.....   | 64 |
| <b>B.1.</b> 3T3 calibration curve obtained by MTS assay.....  | 65 |

## LIST OF ABBREVIATIONS

|               |   |
|---------------|---|
| 2-D:          | Two dimensional   |
| 3-D:          | Three dimensional   |
| ALK:          | Automated lamellar keratoplasty   |
| DMEM:         | Dulbecco's Modified Eagle Medium  |
| ECM:          | Extracellular matrix  |
| FBS:          | Fetal bovine serum  |
| FDA:          | United States Food and Drug Administration  |
| LASIK:        | Laser in situ keratomileusis  |
| MTS:          | 3-(4,5-dimethylthiazol-2-yl)-5-(3-carboxymethoxyphenyl)-2-(4-sulfophenyl)-2H-tetrazolium,(Owen's reagent) |
| PBS:          | Phosphate buffer saline   |
| PGA:          | Poly(glycolic acid)   |
| PHA:          | Poly(hydroxyalkanoate)  |
| PHBV:         | Poly(3-hydroxybutyric acid- <i>co</i> -3-hydroxyvaleric acid)   |
| pHEMA:        | Poly(2-hydroxyethyl methacrylate)   |
| PLGA:         | Poly(lactide- <i>co</i> -glycolic acid)   |
| PLLA:         | Poly(L-lactide- <i>co</i> -D, L-lactide)  |
| PRK:          | Excimer laser photorefractive keratectomy   |
| RGD:          | Arginine-Glycine-Aspartic acid  |
| SEM:          | Scanning electron microscope  |
| TCPS:         | Tissue Culture Polystyrene  |
| Trypsin EDTA: | Trypsin-ethylenediamine tetraacetic acid  |
| UV:           | Ultraviolet   |

# CHAPTER 1

## INTRODUCTION

### 1.1. Tissue Engineering

In recent years the field of biomaterials developed in a new direction involving use of cells and biodegradable carriers called tissue engineering. Tissue engineering is an interdisciplinary biomedical field that aims to produce substitutes that could replace injured or diseased tissues, by using biomaterials, extracellular matrix components and cells (Langer and Vacanti, 1993). General approach in tissue engineering is to harvest cells from the tissue, proliferate them in vitro and seed on an appropriate carrier which can mimic the natural extracellular matrix (ECM) in terms of providing cell attachment, proliferation, migration and function. When this construct of carrier and cell is matured to a certain extent the construct is implanted. Over time, the carrier used degrades in the body, leaving only the cells and the natural ECM, blood vessels etc. produced by them (Freyman et al., 2001).

#### 1.1.1. Components in Tissue Engineering

##### 1.1.1.1. Carriers

Eukaryotic cells are anchorage dependent, therefore, they need a surface to attach. In tissue engineering, polymers of natural or synthetic origin are usually used to provide this surface. These carriers can be 2 or 3 dimensional. The 2 dimensional

carriers are generally in the form of membranes or films and the 3 dimensional ones are mostly foams or sponges of different porosity.

In some studies, the carrier does not only provide the attachment surface but also acts as the reservoir for bioactive molecules like hormones or growth factors just like the natural ECM (Quirk et al., 2004).

The surfaces of these carriers have been modified in many different ways since the beginning of the tissue engineering discipline basically because the cells do not like the synthetic originated polymeric surfaces that do not have the appropriate sequences for cells to attach and are hydrophobic in nature. Therefore, one of the first attempts to modify the surface of the carriers for enhancing cell adhesion rate was to increase surface hydrophilicity by O<sub>2</sub> plasma treatment (Tezcaner et al., 2003) or coating the surfaces with other molecules which are more hydrophilic or contain the appropriate sequences (RGD sequences) for cells to attach (Vleggeert-Lankamp et al., 2004). These methods improved the initial cell attachment and also the proliferation of the cells.

A novel approach to modify the surfaces of the carriers is to use physical or chemical guidance for mimicking the natural tissue in order to increase the organization and the tissue formation rate of the construct and improve the functionality of the newly formed tissue.

In physical guidance, surface topography is used to orient the cells in accordance with physical restraints and, by this way obtain aligned cells. Since the morphology also affects the functionality of the cells, obtaining cells with morphologies close to their natural morphology is important (Walboomers and Jansen, 2001).

The main approach to chemical guidance is to adhere molecules containing RGD sequences and other cell adhesive molecules or molecules that increase hydrophilicity in predetermined pattern on surfaces that do not have these properties, and obtain cell guidance (Schmalenberg et al., 2004).

#### **1.1.1.1.1. Natural Origin**

##### **1.1.1.1.1.1. Collagen**

Collagen is the major protein in mammals constituting 20-30 % of the total body proteins (Harkness, 1961). Since it is a natural molecule, it is biodegradable and biocompatible. Also, since it is a part of the natural ECM it has the signal molecules for cell attachment. It can be found in large amounts from various sources compared to other natural materials used in biomedical field, but obtaining in pure form (pure Type I, II etc.) is very costly (Lee et al., 2001).

##### **1.1.1.1.1.2. Polyhydroxyalkanoates (PHA)**

PHA are intracellular energy and carbon storage products found in various microorganisms and after genetic modification, in plants. In pure form they are biodegradable and biocompatible, therefore, are being used in biomedical applications including tissue engineering (Neuenschwander and Hoerstrup, 2004, Williams et al., 1999). The most commonly used PHA is poly(3-hydroxybutyrate) (PHB) which can be produced by a variety of bacterial strains in large amounts. Among the PHA, copolymers of 3-hydroxyvalerate and 3-hydroxy butyrate are found in different ratios (PHBV) and are within the most studied (Tezcaner et al., 2003, Torun Köse et al., 2003, Li and Chang, 2005).

##### **1.1.1.1.2. Synthetic Origin**

Constructing carriers from synthetic originated polymers have advantages of large scale production and processing. They have to be prepared under strictly controlled polymerization conditions and extensively purified of the catalysts, initiators and unreacted monomers. They, like PHA, lack the signals that can be recognized by cells for attachment, therefore, in most cases their surfaces need to be modified to increase the attachment efficiency of cells.

Most commonly used synthetic polymers in biomaterials in general and specifically in tissue engineering are polyesters, namely poly(L-lactic acid) (PLLA), poly(glycolic acid) (PGA) and poly(lactide-*co*-glycolic acid) (PLGA). They are approved by the United States Food and Drug Administration (FDA) for human clinical use (Langer, 2000). All its copolymers are biodegradable and biocompatible. The hydrolytic degradation product of PLLA is lactic acid which goes into the tricarboxylic acid cycle in the cell and excreted as CO<sub>2</sub> and H<sub>2</sub>O from the body. Similarly, PGA undergoes hydrolysis and other degradative reactions which include enzymatic degradation by nonspecific esterases or carboxypeptidases and yields glycolic acid. Glycolic acid can enter to tricarboxylic acid cycle or excreted from the body through urinary system (Chen et al., 2002). PLGA is the copolymer of lactic and glycolic acids. Its properties like degradation rate or mechanical strength can be altered by changing the ratio of lactic acid to glycolic acid in the copolymer (Kim and Mooney, 1998).

#### **1.1.1.2. Cells**

The cells used in tissue engineering are specific to the tissue targeted for regeneration and can be derived from different sources. The ideal cell source for this purpose is the autologous cells, own cells of the organism that needs the regeneration (patient or experimental animals). The main advantage of usage of mature autologous cells is the prevention of the risk of immunological response. However, availability of these cells is limited and cause pain, also has risk of infection. In such cases different cell sources such as stem cells, allogenic cells or xenogenic cells should be considered (Nishida et al., 2004, Buma et al, 2004). The usage of stem cells in tissue engineering is a novel and promising approach since these cells can differentiate into different cell types with stimulation and they have a higher proliferative capacity. But their utilization depends on and are limited with the stem cell researches (Sun et al., 2005). Allogenic cells are the cells from a different individual of the same species. Their use is limited due to immunogenic response (rejection) caused by them (Niemeyer et al., 2004).

Xenogenic cells are cells from other species rather than the target organism. Their use is not frequent since they can induce severe inflammatory and immunological responses leading to rejection by the tissue or transmission of infectious diseases. Instead, the xenogenic-origin materials are generally used as acellular matrix materials for autologous cell seeding or are prevented from direct contact with tissue (Leyh et al., 2003, Teebken et al., 2000).

## **1.2. Cornea Engineering**

Corneal injuries constitute approximately 37 % of all visual disabilities and 23% of medical visits for ocular problems in North America. They can be superficial with damage limited to the epithelium (such as in uncomplicated erosion) or associated with a deeper involvement of the epithelial basement membrane, the stromal lamella and even endothelium (the inner most layer). Cause of these injuries can be recurrent erosion, mild chemical burns, superficial herpetic infections, neuroparalytic cornea, autoimmune diseases, and stromal ulcerations due to viral or bacterial infections or severe burns (Reim et al., 1997). Despite currently available treatments, corneal scar tissue formation occurs in many of these injuries. Corneal scar tissue formation is a very severe problem which leads to loss of transparency of the cornea and eventually leads to blindness. In such cases, replacement of cornea is necessary. For corneal replacements, donor corneas and artificial corneas have been used but both have some drawbacks (Moticka and She, 1989, Lau et al., 1998, Hicks et al., 1997). The current research on corneal treatments focus mainly on tissue engineering of cornea which will be a very promising method if succesful.

### **1.2.1. Function and Structure of the Cornea**

There are two primary functions of the cornea. First of all, it protects the rest of the eye from foreign materials with the help of sclera, tears and eyelids. It also prevents the passage of some of the most damaging ultraviolet (UV) wavelengths in sunlight (180 to 315 nm). It also functions as the eye's outermost lens by contributing

65 to 75 % of light focusing. Cornea refracts the incoming light onto the lens and the lens refocuses that light onto the retina, the light sensitive layer of cells lining the posterior chamber. The retina then translates the incoming light into impulses which are then sent to the brain through the optic nerve and the vision occurs (Chirila et al., 1998).

The cornea is the eye's outermost layer (Fig. 1.1). It is approximately 500  $\mu\text{m}$  in thickness (Ehlers and Hjortdal, 2004). To refract light properly it must be transparent. Although it is transparent, corneal tissue consists of highly organized group of cells and ECM. Reasons of corneal transparency has been investigated for many years (Maurice, 1957, Hogan et al., 1971, Ameen et al., 1998). Key factor appears to be the unique structure of its ECM, the collagen fibers of which have a highly regular arrangement. They alternate as orthogonally oriented lamellae especially in the central and posterior stroma (Fig. 1.2). This arrangement is influenced by the degree of hydration. The proteoglycans (keratan sulphate, chondroitin sulphate and dermatan sulphate) in the ECM also participate in this regular arrangement (Müller et al., 2004).

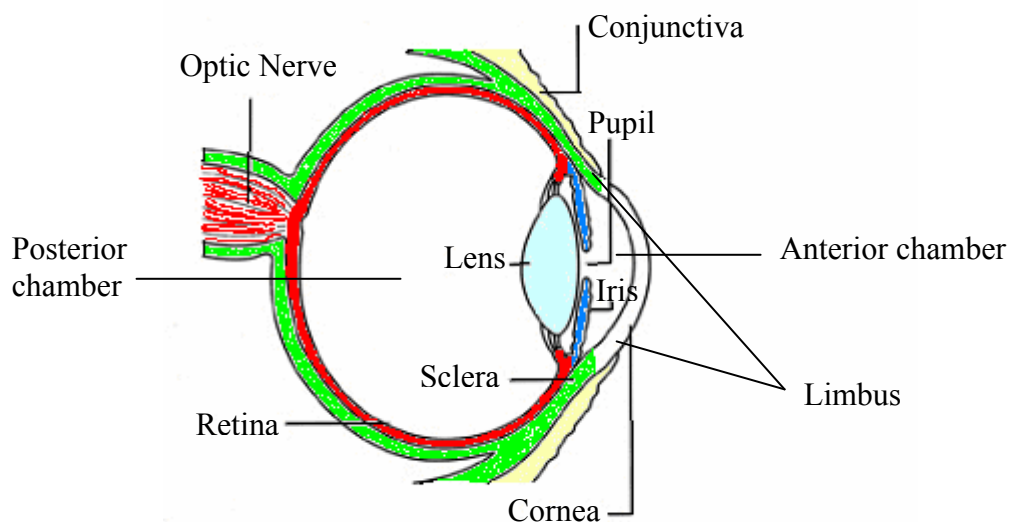


**Figure 1.1.** Structure of the eye.

Central cornea is devoid of blood vessels and this helps to maintain transparency. Therefore, cornea receives its nourishment from the tears that wash its surface and from the aqueous humor that fills the anterior chamber behind it (Cursiefen et al., 2003).

The corneal tissue is arranged in five basic layers, each having an important function. These layers (from the outside towards inside) are epithelium, Bowman's layer, stroma, Descemet's membrane and endothelium (Fig. 1.3).

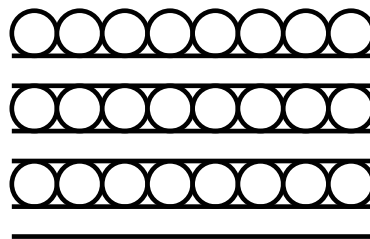


**Figure 1.2.** Orthogonal orientation of collagen fibers in the corneal stroma.

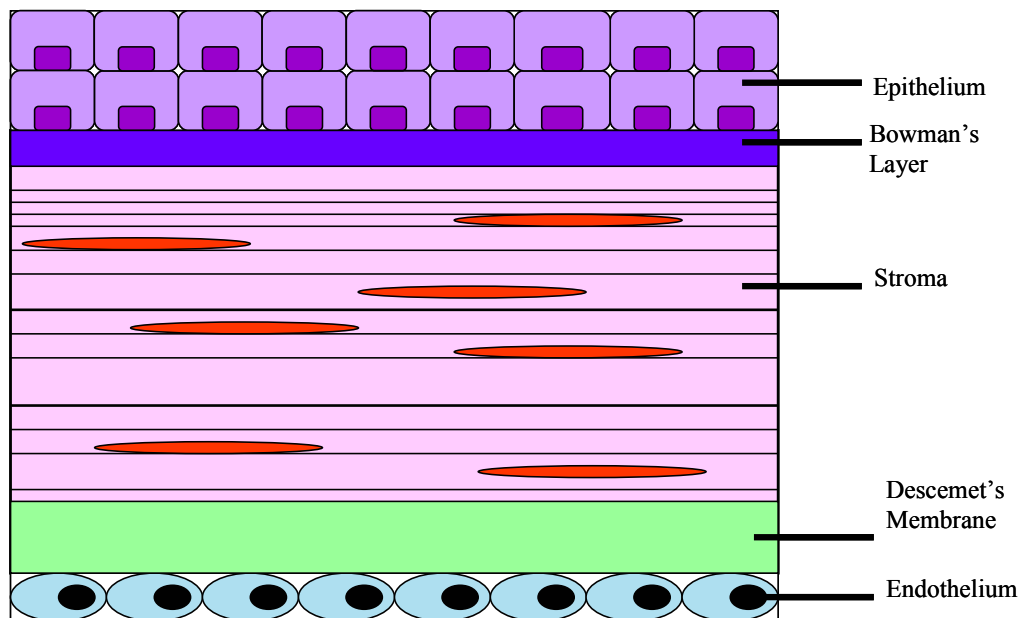


**Figure 1.3.** Layers of the cornea.

Epithelium is the outermost layer which is about 10 % of the cornea's thickness. The basic function of the epithelium is to coordinate the passage of materials in and out of the cornea. It prevents passage of foreign materials like dust and microorganisms, while providing the surface for adsorption of nutritional elements from the tears. The corneal epithelium is a nonkeratinizing, stratified squamous epithelium which consists of five cell layers centrally and up to 10 cell layers peripherally. Cells in the first layer are polygonal and become more flattened towards the top layers. These cells anchor to and organize themselves on the basement membrane that they secrete (Hogan et al., 1971, Kivela and Uusitalo, 1998).

Bowman's layer is a transparent sheet composed of layered collagen located just below the basement membrane of the epithelium.

The layer which constitutes 90 % of the corneal thickness is the stroma. It is populated with fibroblastic cells called keratocytes. It consists mainly of water (78 %) and collagen (16 %). The collagen in the stroma gives the cornea its strength, elasticity, and form (Michelacci, 2003).

Descemet's membrane is located between the stroma and the endothelium of the cornea. It is composed of collagen fibers and serves to protect the inner layers from infections and injuries. Descemet's membrane is secreted by the endothelial cells that lie below it.

The endothelium is the innermost layer of the cornea. It consists of monolayer of polygonal endothelial cells. The corneal endothelium is very different than the vascular endothelium. Its primary function is that of a pump. In the normal cornea, there is a fluid leakage from the anterior chamber into the stroma of the cornea. If this leakage is not prevented, the stroma would swell and lose its transparency. On the otherhand, if stroma is dehydrated excessively, the arrangement of collagen fibers would disturbed resulting again in the loss of transparency. Therefore, in a healthy eye, endothelium maintains the balance between fluid passage with its pumping action (Engelmann et al., 2004).

### **1.2.2. Diseases and Disorders Affecting the Cornea**

Refractive errors are the most common of all vision problems and affect about 120 million people only in the United States (National Eye Institute, 2004). Refractive errors are caused by irregularly shaped cornea which causes light to be transmitted imperfectly on the retina resulting in poor vision. If the curvature of the cornea is too high, the disorder caused by this is called myopia. The light focused falls in front of the retina and distant objects can not be seen clearly. If the curvature of the cornea is too low then the light is focused beyond the retina and the disorder is called hyperopia. The objects close to the patient can not be seen sharply. Astigmatism is caused by the uneven curvature of the cornea and the image formed is blurred for both distant and near objects. Eyeglasses or contact lenses are generally used to correct these refractive errors. Also, refractive surgeries such as excimer laser photorefractive keratectomy (PRK), automated lamellar keratoplasty (ALK) and laser in situ keratomileusis (LASIK), are being commonly used worldwide (Fantès et al., 1990, Moller-Pedersen et al., 1998).

Corneal damages caused by foreign material penetrations or contamination of cornea by bacteria or other pathogens can lead to corneal infections or inflammations called keratitis. These imperfections can disturb visual clarity or may erode the cornea. Corneal infections can also lead to corneal scarring, which can impair vision. The deeper the corneal infection the more is the severity of the symptoms and complications (Remeijer et al., 2004, Walochnik et al., 2003).

Corneal injuries can be superficial or penetrating according to the nature of the damage. Superficial corneal injuries, so called corneal abrasions, can be caused by foreign materials such as sand or dust, overuse of contact lenses or exposure to ultraviolet radiation. Penetrating corneal injuries are much more serious and can be caused by high speed particles, chemical burn by strong acids or alkali, and penetration of objects. Blurred vision, abnormal sensitivity to light, pain, redness, swollen eyelids are the symptoms of the corneal injury (Aziz and Rahman, 2004, Schrage et al., 2000).

Cornea has the ability to heal itself in simple corneal infections or injuries. Generally, the eye is covered to prevent further damages and antibiotic drops or ointments are used to enhance the healing. Severe corneal injuries may require extensive surgery or even corneal replacements.

### **1.2.3. Corneal Response to Injury**

The cornea can heal itself very rapidly after minor injuries or abrasions by sliding of the healthy cells quickly and patching the injured site before infection occurs and vision is affected. Therefore, the repair of the corneal tissue requires cell migration, adhesion, and proliferation. Cell adhesion and migration depend on the synthesis and arrangement of the ECM by the cells. Healing of the cornea is mainly related to the epithelial layer of the cornea. Along with the epithelial cells, stromal keratocytes play an important role in corneal healing process. Corneal injury has been reported to induce a series of phenotypic changes resulting in the transformation of stromal keratocytes into a fibroblastic cell type that has similarities with the myofibroblasts (Jester et al., 1999). Corneal wound healing is a complex process that results in scar tissue formation. The most important criteria in corneal healing is the restoration and maintenance of the transparency of the cornea. For more serious corneal injuries like penetrating injuries, the scar tissue formed as a consequence of healing process could be so large that the transparency could not be restored. In severe cases like these, corneal replacements are necessary to prevent blindness.

### **1.2.4. Approaches for Severe Corneal Damages**

#### **1.2.4.1. Corneal Transplantation**

When the cornea is injured so severely that the transparency of it is lost mainly due to scar tissue formation, it is mostly not possible to restore the vision with any treatment including corrective surgeries that can be performed by laser. In

cases like these, replacement of the cornea is needed. Today, most widely used treatment for corneal replacements is corneal transplantation (Shimmura, 2004).

Corneal transplant surgery is a complicated procedure, and full recovery can take from a few months up to a year in some cases. Drugs are used to enhance healing and prevent rejection of the foreign tissue. One of the advantages of corneal transplantation is that the rejection of the transplanted tissue is very rare seen in contrast to high rejection rate observed with other organ transplants. Due in part to that the cornea is an immune-privileged tissue because of its avascularity, corneal transplants require only local immune suppression and represent the most successful transplants.

There are, however, drawbacks of corneal transplantation, too. Although there is a relatively low rejection rate, primary immune rejection is still a problem. Variability of the quality of the donor tissue also causes inconsistencies in their success rate. Furthermore, eyes treated with corrective surgeries are unacceptable for future donations. Also, as with any other transplantation, transmission of diseases is a problem. Finally, donor shortage is the main problem and there is an unmet need of donor corneas for blind people worldwide (Nishida, 2003).

#### **1.2.4.2. Keratoprotheses**

Keratoprotheses are artificial corneas. Researchers have tried to develop a permanent artificial cornea for patients who had severe corneal damages and could not have corneal transplantation because of donor scarcity or inability to retain corneal transplants. Initial clinical results using poly(2-hydroxyethyl methacrylate) (pHEMA) have been promising but problems with mechanical weakness and calcium deposition have yet to be solved (Chirila et al., 1998). One of the major developments of design in this field has been the use of porous skirts around a transparent hydrogel center (Chirila, 2001). These materials have been shown to allow ECM accumulation. However, there remain complications that result in the failure of keratoprosthetic devices, such as the lack of epithelial coverage in front of

the artificial cornea. The absence of a continuous sheet of epithelium permits bacterial invasions, inhibits the spreading of an even tear film, and causes epithelial downgrowth (Latkany et al., 1996). The keratoprotheses do not contain viable elements, and the current designs require significant improvement.

#### **1.2.4.3. Tissue Engineering**

Isolation and cultivation of the cells that a tissue comprises, is the first step to produce that tissue in vitro. This step is very important since the quality of the engineered tissue depends highly on the quality of the cells used to reconstruct it. The ideal cells used for tissue engineering should have extensive proliferation potential and suitable differentiation abilities. As discussed above, cornea is composed of three cell types: epithelial cells, keratocytes and endothelial cells.

The corneal epithelium is a self-renewing tissue, therefore, it contains stem cells. The stem cells of the corneal epithelium are not uniformly distributed on its surface. They are restricted to the limbus part which is a transition zone between cornea and conjunctiva (Kruse, 1994). During corneal healing, it is thought that, the limbal epithelial cells move to the basal layer of the central cornea and then move through the stratified epithelium toward the surface (Thoft and Friend, 1983). The cells from the basal layer of the central cornea are transient cells and can proliferate for a limited number of divisions. In contrast, the cells of the limbus have the proliferative characteristics of stem cells as they are cycling slowly (Cotsarelis et al., 1989). These cells, therefore, could be used for tissue engineering purposes. Corneal or limbal cells can be isolated by enzymatic digestion. The cultivation of these cells on irradiated fibroblasts was found to be an adequate method since it promotes epithelial cell proliferation by limiting the outgrowth of keratocytes by contact inhibition, that may be isolated along with epithelial cells (Lindberg et al., 1993).

Keratocytes can be isolated from the corneal stroma by removing the epithelium and treating the stromal explants enzymatically to obtain single cells. Also, keratocytes can be obtained from the keratocyte contamination in epithelial cell

cultures by changing the ingredients of the medium for keratocytes. Epithelial cells are lost during the passages since this medium is not appropriate for them to proliferate (Germain et al., 2000).

Endothelial cells can be isolated from the endothelial layer of the cornea. Isolation of these cells is difficult since they show very high adherence to their ECM which is the Descemet's membrane. The usual enzymatic treatment with trypsin in cell isolation, can not be used in isolation of endothelial cells as it leads to degradation of the cells due to long incubation times to obtain detachment. Since the Descemet's membrane consists of mainly collagen, treating with collagenase is a better approach. As in the isolation of corneal epithelium cells, isolation of sufficient numbers of endothelial cells and removal of the stromal keratocytes which contaminate the culture because of the isolation technique are important issues. The keratocytes can be eliminated by using selective medium which contains D-valine instead of L-valine because the fibroblastic cells can not convert the D-form of the amino acid into the L-form, which is necessary for them to survive (Engelmann et al., 2004).

Since the cornea is composed of three different cell populations, researchers are generally focused on reconstructing one or at most two layers of the cornea. Several corneal tissue models have been produced in vitro using animal corneal cells. Rabbit corneal equivalents were constructed by culturing rabbit corneal epithelial cells on rabbit stromal keratocytes within a collagen gel (Zieske et al., 1994). In other studies, human conjunctival epithelial cells were seeded on collagen gels alone or co-cultured with human conjunctival fibroblasts or fibroblasts from other species (Tsai and Tseng, 1994, Tsai et al., 1994).

In the first attempt to produce a corneal equivalent with human cells, epithelial and stromal layers of the cornea were constructed, however the Descemet's and Bowman's membranes and the endothelium were absent (Germain et al., 2000). The stromal tissue was reconstructed by combining human corneal keratocytes with bovine type I collagen which was achieved as a collagen gel in which keratocytes were dispersed. After culturing the keratocytes for 4 days, human limbal epithelial cells were seeded on mature reconstructed stroma. By changing the culture medium

with epithelial growth factor (EGF), insulin, hydrocortisone, cholera toxin and serum which were necessary for epithelial cells, coverage of the stromal surface with epithelial cells was obtained. After incubation for 3 days submerged in the medium, the epithelial cells had formed multilayers just like the natural cornea. The thickness of the reconstructed cornea was close to that of natural one and it was transparent which is the most important criteria for functionality of the cornea.

The reconstruction of corneal endothelium was made but this was not combined with other reconstructed layers of cornea except in one study where the three cell types of bovine origin were used (Minami et al., 1993). It is very difficult to construct a properly functioning “full thickness” cornea with all three layers. During the recent years, several groups have attempted to construct a full thickness human cornea using cultured cells (Griffith et al., 1999, Mimura et al., 2004). Major problems with these reconstructed corneas were stability and absence of function. Researchers used the reconstructed endothelium layers with donor corneas which are not suitable for transplantation because of the absence of this layer. This is indeed very important because today in the western world most corneal surgeries are performed by using donor corneas which are prepared and cultured by The European Cornea Banks (approximately 25 000 corneas per year), of which only 60% meet the quality criteria and can be used for corneal surgeries. The remaining 40% can not be used mainly because of their low endothelial cell density (European Eye Bank Directory, 2003). Also, in the USA among the 35 000 corneal transplants performed each year is only the 60% of the total donated corneas per year (Beck et al., 1999).

In this study, polymeric carriers of PLLA and PHBV8 were designed for the reconstruction of epithelial and the stromal layers of the cornea. These carriers were tested in vitro for their physical properties and for their compatibility with the cells. The results showed that the carriers designed permit cell proliferation and functionality, therefore, they could be used as carriers for the tissue engineering of the cornea after further developments.

## CHAPTER 2

### MATERIALS AND METHODS

#### 2.1. MATERIALS

Poly(3-hydroxybutyric acid-*co*-3-hydroxyvaleric acid) (PHBV8, HV content 8 w/w %) was purchased from Aldrich Chemical Company, Inc. (USA). Poly(L-lactide-*co*-D, L-lactide) (PLLA, RESOMER® LR 708, Molar ratio L-lactide: D, L-lactide 70:30) was supplied by Boehringer Ingelheim Pharma GmbH & Co. KG. (Germany). Fetal bovine serum (FBS) was obtained from Biochrome KG (Germany). Dulbecco's Modified Eagle Medium (DMEM) was obtained from Gibco Invitrogen Corporation (New Zealand). MTS kit was purchased from Promega Corporation (USA). Cacodylic acid (sodium salt), ascorbic acid, glutaraldehyde (Grade I, 25 % aqueous solution), trypsin-EDTA (0.25 %), monoclonal anti-collagen type I (clone col-1, mouse ascites fluid) and monoclonal anti-pan cytokeratin (mixture clones C-11, PCK-26, CY-90, KS-1A3, M20, A53-B/A2, mouse ascites fluid) were supplied by Sigma Chemical Corporation (USA). Mouse anti-ZO-1 was purchased from Zymed Laboratories Inc. (USA). Formaldehyde (37 %), dichloromethane (DCM) and dioxane were obtained from Merck KGaA (Germany). Fibronectin (FN pure, from human plasma) was purchased from Roche Diagnostics (Germany). AlexaFluor 488 was supplied by Molecular Probes Inc. (USA). Acridine Orange was obtained from BDH Chemicals Ltd. (UK). The RPE cell line D407 was a personal gift of Dr. R.Hunt (Department of Ophthalmology, University of South Carolina Medical School, Columbia, SC., USA). 3T3 cell line was purchased from Foot-and-Mouth Disease Institute of Ministry of Agriculture & Rural Affairs (Turkey). Human

osteoblast like-Saos-2 cells (derived from osteosarcoma) are obtained from American Type Culture Collection ATCC no. HTB 85.

## 2.2. METHODS

### 2.2.1. Preparation of Carriers

#### 2.2.1.1. Preparation of Micropatterned Films

Micropatterned silicon templates with different dimensions and geometries (Fig. 2.1, Table 2.1) were produced by photolithography and subsequent chemical etching (courtesy of Prof. A. Aydınlı and İ. Kıyat, Bilkent University).

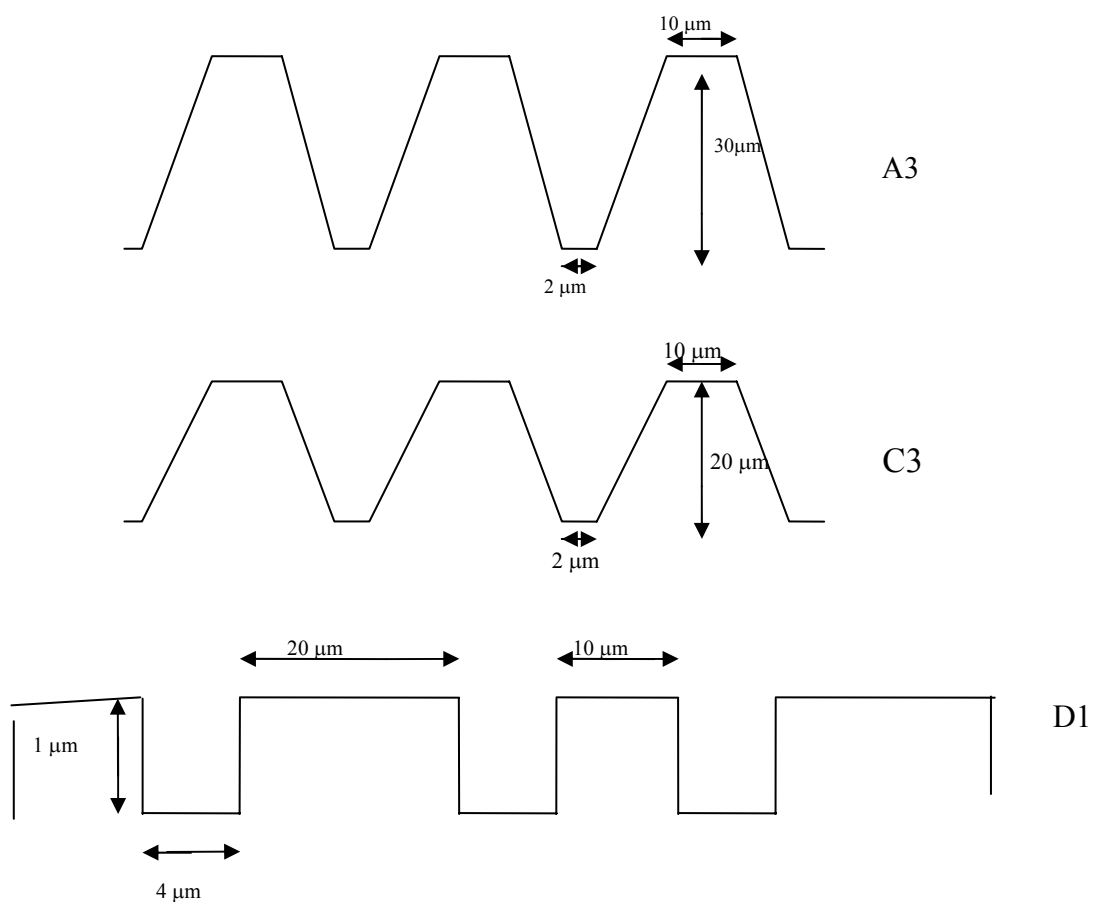


**Figure 2.1.** Cross-section of A3, C3 and D1 templates.

**Table 2.1.** Dimensions and geometry of micropatterned templates.

| Template | Geometry of template    | Groove width ( $\mu\text{m}$ ) | Ridge width ( $\mu\text{m}$ ) | Groove depth ( $\mu\text{m}$ ) |
|----------|-------------------------|--------------------------------|-------------------------------|--------------------------------|
| A3       | Parallel channels       | 2                              | 10                            | 30                             |
| C3       | Parallel channels       | 2                              | 10                            | 20                             |
| D1       | Alternating square pits | 4                              | 20 /10                        | 1                              |

Films were prepared by solvent casting PLLA-PHBV8 (1:1) in DCM ( 4 %) solution onto the micropatterned template.

#### **2.2.1.2. Preparation of Foams**

PLLA-PHBV8 (1:1 w/w) in dioxane (4 %, 45 ml) solution was poured into glass Petri dishes (dia. 10 cm) and maintained at  $-20^{\circ}\text{C}$  overnight. The frozen polymer solution was freeze dried (FreeZone<sup>®</sup> 6 Liter Freeze Dry System, Labconco Corporation, USA) for 16 h.

#### **2.2.1.3. Preparation of Three Dimensional (3-D) Micropatterned Cell Carriers**

Micropatterned film material was added to the patterned template as described in Section 2.2.1.1 and an already prepared foam was placed on top of the evolving film before its solvent evaporated completely. Thus, the foam and the film were attached to each other and a 3-D, surface-patterned construct was formed.

## 2.2.2. Characterization of Carriers

### 2.2.2.1. Physical Characterization

Foam density was calculated by using a pycnometer ( $n = 2$ ). An empty pycnometer was weighed ( $W_0$ ). It was weighed again after completely filling with water ( $W_1$ ). Then, a previously weighed ( $W_f$ ) foam was placed in the pycnometer which was then filled with dH<sub>2</sub>O and weighed again ( $W_2$ ). The addition of foam displaced equal amount of water. However, during this process some amount of water was adsorbed by the foam because of its porous structure and capillary action. Therefore, the foam was weighed again ( $W_3$ ) after removal from the pycnometer. All these data were used to calculate the volume of the foam that was used to calculate the density of the foam as described below.

$$W_{w1} = W_1 - W_0 \quad \text{Weight of water completely filling the pycnometer}$$

$$W_{w2} = W_2 - W_f - W_0 \quad \text{Weight of water remaining inside after foam was placed}$$

$$W_r = W_{w1} - W_{w2} \quad \text{Weight of water displaced by the foam}$$

$$V_w = W_r + (W_3 - W_f) \quad \text{Volume of displaced water which is equal to its displaced weight}$$

$$V_w = V_f$$

$$D_f = W_f / V_f$$

The thickness of the films, foams and 3-D construct were measured by a micrometer with a 0.001 mm sensitivity ( $n = 6$ ).

### **2.2.2.2. Microscopic Characterization**

The topography of the carriers were studied using a Scanning Electron microscope (SEM) (JSM 6400, JEOL, Japan) after coating with a thin film of gold, under vacuum.

The cross-section of the foams was examined under a light microscope (IX 70, Olympus, Japan) after taking 4 or 10  $\mu\text{m}$  thick sections by using a frozen microtome (CM 1510, Leica, Germany).

### **2.2.3. Cell Culture Studies**

#### **2.2.3.1. Saos-2 Cells**

The 3-D constructs were sterilized by treating with sterile EtOH (70 %, prepared with absolute EtOH and sterile distilled water) for 2 h and then washed 4 times with PBS (10 mM, pH 7.3). Saos-2 cells (osteosarcoma cells) were seeded as model cells. Out of the 6 specimens, 2 were seeded on the film side, 2 were seeded on the foam side and 2 were seeded on both sides. The seeding density was 500 000 cells/20  $\mu\text{l}$  for foam side and 50 000 cells/20  $\mu\text{l}$  for film side. 3-D constructs were incubated at 37  $^{\circ}\text{C}$  in a carbon dioxide incubator (5 %  $\text{CO}_2$ , MCO-17AIC, Sanyo Electric Co. Ltd., Japan) for 1 week and the medium (Dulbecco's Modified Eagle Medium (DMEM) supplemented with 5 % fetal bovine serum (FBS), 100 units/ml penicillin and 100 units/ml streptomycin) was changed periodically everyday. At the end of 1 week, the specimens were fixed with glutaraldehyde (2.5 %) for 2 h, washed twice with cacodylate buffer (0.1 M, pH 7.4) and prepared for SEM.

## **2.2.3.2. D407 (Retinal Pigment Epithelial Cell Line) and 3T3 Cells**

### **2.2.3.2.1. Cell Culture**

D407 cells (passage 5 to 15) and 3T3 cells (passage 5-15) were cultivated in high glucose DMEM supplemented with 5 % fetal bovine serum FBS, 100 units/ml penicillin and 100 units/ml streptomycin at 37 °C in a carbon dioxide incubator (5 % CO<sub>2</sub>, MCO-17AIC, Sanyo Electric Co. Ltd., Japan). The cells were passaged using 0.05 % trypsin-EDTA solution.

### **2.2.3.2.2. Cell Seeding onto Carriers**

#### **2.2.3.2.2.1. Micropatterned Films**

In the cell seeding tests some films were used with fibronectin treatment while others were used as is. PLLA-PHBV8 films were sterilized by immersing in sterile EtOH (70%) for 2 h at 4 °C. The films were then washed 4 times with PBS. They were then placed into 24-well plates and coated with fibronectin by incubating in fibronectin solution for 10 min (50 µg/ml fibronectin in PBS). At the end of 10 min, the films were washed with PBS to remove excess fibronectin and dried under sterile conditions in a laminar flow (LaminAir Safe 2000, Holten A/S, Denmark). D407 cells were detached from the tissue culture flasks by using 0.05 % trypsin for 5 min at 37°C, then centrifuged for 5 min at 3000 rpm and resuspended in high glucose DMEM supplemented with 5 % FBS, 100 units/ml penicillin and 100 units/ml streptomycin. Cell number was counted using NucleoCounter (ChemoMetec A/S, Denmark). 50 000 cells/20 µl were seeded on each film and the films were not disturbed for 30 min to allow cell attachment. After 30 min, 500 µl high glucose DMEM supplemented with 5 % FBS, 100 units/ml penicillin and 100 units/ml streptomycin were added. They were incubated in a CO<sub>2</sub> incubator (5 % CO<sub>2</sub>, 37 °C) for 14 days. The medium was refreshed every day. Tissue culture polystyrene (TCPS) was used as the control.

#### **2.2.3.2.2.2. Foams**

PLLA-PHBV8 foams were sterilized by immersing in sterile EtOH (70 %) for 2 h at 4 °C. The foams were then washed 4 times with PBS. After coating with fibronectin overnight and washing with PBS, the foams were placed into 24-well plates. The 3T3 cells were detached from the tissue culture flasks by incubating in 0.05 % trypsin-EDTA for 5 min at 37 °C. The cell suspension was centrifuged for 5 min at 3000 rpm and resuspended in high glucose DMEM supplemented with 5 % FBS, 100 units/ml penicillin and 100 units/ml streptomycin. Cell number was counted in NucleoCounter. Two different seeding densities were used; 500 000 cells/75 µl or 250 000 cells/75 µl were seeded on each foam and the foams were not disturbed for 45 min to allow cell attachment. After 45 min, 500 µl high glucose DMEM with 5 % FBS, 100 units/ml penicillin and 100 units/ml streptomycin were added. They were incubated in a CO<sub>2</sub> incubator (5 % CO<sub>2</sub>, 37 °C) for 14 days. The medium was refreshed every day. After 7 days of incubation, the number of medium refreshments per day was increased to 2. Tissue culture polystyrene (TCPS) was used as the control because of its optimal properties for cell cultivation.

#### **2.2.3.2.2.3. 3-D Constructs**

The 3-D, surface-patterned foam-film constructs were sterilized by immersing in sterile EtOH (70 %) for 2 h at 4 °C. They were then washed 4 times with PBS and placed into 24-well plates. Since there was both a film side and a foam side, coating with fibronectin was done as follows; first the film foams were incubated in 500 µl of fibronectin solution for 10 min and then half that solution was removed leaving only the foam side in contact with the fibronectin for 2 h. The construct was then washed with PBS.

The D407 cells were detached from the tissue culture flasks by incubating in 0.05 % trypsin-EDTA for 5 min at 37 °C. The cell suspension was centrifuged for 5 min at 3000 rpm, resuspended in high glucose DMEM supplemented with 5 % FBS,

100 units/ml penicillin and 100 units/ml streptomycin. Cell number was counted using Nucleocounter. 50 000 cells/20  $\mu$ l was seeded on the film side and the constructs were not disturbed for 30 min.

The 3T3 cells were detached from the tissue culture flasks by incubating in 0.05 % trypsin for 5 min at 37  $^{\circ}$ C. The cell suspension was centrifuged for 5 min at 3000 rpm and resuspended in high glucose DMEM supplemented with 5 % FBS, 100 units/ml penicillin and 100 units/ml streptomycin. Cell number was counted using Nucleocounter. The foam-films were then turned upside down for seeding into foam side. 250 000 3T3 cells/75  $\mu$ l was seeded on the foam side and returned to its normal position (film side up). The constructs were not disturbed for 45 min. To prevent dehydration of the cells seeded on the film side during this 45 min, 20  $\mu$ l medium was added only on the top of the films. At the end of 45 min, 500  $\mu$ l high glucose DMEM supplemented with 5 % FBS, ascorbic acid (50 $\mu$ l/ml, 0.3 mM), 100 units/ml penicillin and 100 units/ml streptomycin were added. Ascorbic acid was added to induce insoluble collagen deposition onto carriers by the 3T3 cells seeded. They were incubated in an CO<sub>2</sub> incubator (5 % CO<sub>2</sub>, 37  $^{\circ}$ C) for 14 days. The medium was refreshed every day. After 7 days of incubation, the number of medium refreshments per day was increased to 2. Tissue culture polystyrene (TCPS) was used as the control.

#### **2.2.3.2.3. Characterization of Cell Seeded Carriers**

##### **2.2.3.2.3.1. D407 Cells**

###### **2.2.3.2.3.1.1. Cell Proliferation**

Cell number was quantified by using MTS assay (Nonradioactive cell proliferation assay, Torun Köse et al., 2003). A calibration curve was constructed using the predetermined cell numbers (counted with NucleoCounter) of D407 cells. 25 000, 50 000, 100 000, 250 000 and 500 000 cells were seeded on 24 well plates in triplicate and incubated for 4 h. The medium was then removed and the sample was

washed with PBS. MTS solution (500 $\mu$ l, 10 % PMS and MTS in DMEM low glucose medium) was added. After 2 h of incubation at 37  $^{\circ}$ C, 100  $\mu$ l of this solution was transferred to a 96-well plate. The optical density (OD) at 490 nm was determined with a kinetic microplate reader (Maxline Vmax<sup>®</sup>, Molecular Devices, USA) and a plot of OD versus cell number was prepared (Appendix I). After seeding the films and 3-D constructs as described in Section 2.2.3.3, the cell number was quantified at predefined time points using the calibration curve for D407 cells. For this, the construct was transferred into a fresh 24-well plate, the construct was washed with PBS and MTS (500  $\mu$ l) solution was added. The cells were incubated for 2 h in the CO<sub>2</sub> incubator and the OD at 490 nm of the aliquots from the wells was measured with kinetic microplate reader. The proliferation curves for D407 cells seeded onto films and foam-films were obtained ( $n = 3$ ).

#### **2.2.3.2.3.1.2. Morphology of Cells**

For SEM and fluorescence microscopy (IX 70, Olympus, Japan) the D407 cells seeded onto films and film sides of the 3-D constructs were first fixed with glutaraldehyde (2.5 %) for 2 h and then washed twice with cacodylate buffer (0.1 M, pH 7.4). SEM specimens were left in the laminar flow overnight for drying and then examined with SEM after coating with gold. The samples to be stained with Acridine orange were washed with HCl (0.1 M) for 1 min and Acridine orange was added. After 15 min, Acridine orange was removed and the sample was washed with distilled water. The cells were observed under the fluorescence microscope at the excitation wavelength of 480 nm.

#### **2.2.3.2.3.1.3. Immunohistochemical Studies**

For immunohistochemical analysis, fixation was done with formaldehyde (4 %) for 30 min, and samples were washed twice with PBS. Triton-X 100 (0.1 %) was used to permeabilize the cells by treating for 5 min and washing 4 times with PBS. After this treatment, the samples were transferred to blocking solution (0.5 % BSA,

0.1 % Tween 20, 0.1 % FBS, 0.1 % sodium azide in PBS) for 30 min. Primary antibodies (250 µl) were added to each well. Mouse anti ZO-1 (15 µg/ml in blocking solution) or Anti-Pan cytokeratin (diluted 200 fold in blocking solution) was pipetted, and the samples were added to these primary antibodies with their patterned side facing downwards and incubated at 4 °C overnight . They were incubated with secondary antibody (Alexaflour 488, 300 µl diluted 400 fold in blocking solution) for 1 h at 37 °C, washed 3 times with PBS and examined under the fluorescence microscope at the excitation wavelength of 480 nm.

### **2.2.3.2.3.2. 3T3 Cells**

#### **2.2.3.2.3.2.1. Cell Proliferation Studies**

Cell number was quantified with MTS assay. A calibration curve for 3T3 cells was constructed as described in Section 2.2.4.1.1 (Appendix II) . After seeding the foams and 3-D constructs with the 3T3 cells as described in Section 2.2.3.3, the cell number was quantified at predefined time points using the calibration curve ( $n = 3$ ).

#### **2.2.3.2.3.2.2. Morphology of Cells**

For SEM and fluorescence microscopy, foams and 3-D constructs were fixed with with glutaraldehyde (2.5 %) for 2 h and then washed twice with cacodylate buffer.

The SEM specimens were dried in a freeze dryer for 8 h and then examined with SEM after coating with gold.

The samples to be stained with Acridine orange for fluorescence microscopy were first sectioned by using a microtome (CM 1510, Leica, Germany). The sections were then washed with HCl (0.1 M) for 1 min and Acridine orange (500 µl) was added. After 15 min, Acridine orange was removed and the sample was washed with distilled water. The microscopic examination was done with the a fluorescence

microscope at the excitation wave length of 480 nm.

### **2.2.3.2.3.2.3. Immunohistochemical Studies**

For immunohistochemical analysis, the samples were fixed by incubating in formaldehyde (4 %) for 30 min and sectioned with the microtome. First, the blocking solution (0.5 % BSA, 0.1 % Tween 20, 0.1 % FBS, 0.1 % sodium azide in PBS) was pipetted onto the sections and incubated for 30 min at room temperature. Then, the primary antibody (monoclonal anti-collagen type I, 250  $\mu$ l) was pipetted on to each section and incubated 2 h at 37 °C. Finally, they were incubated with secondary antibody (Alexaflour 488, 300  $\mu$ l, diluted 400 fold in blocking solution) for 1 h at 37°C , washed 3 times with PBS and examined under the fluorescence microscope (IX 70 Olympus, Japan) at the excitation wavelength of 480 nm.

## CHAPTER 3

### RESULTS AND DISCUSSION

#### 3.1. Physical and Microscopic Characterization of Films and Foams

In this study a variety of biodegradable, polymeric cell carriers of 2-D (films) and 3-D (foams and film-foams) form were designed. The polyesters used in the construction were PLLA and PHBV8, both well known biomedical materials. The carriers were characterized before testing in vitro.

##### 3.1.1. Foam Density

The density of PLLA-PHBV8 foams was calculated as  $0.1045 \pm 0.03$  g/ml by using a pycnometer ( $n = 2$ ). This low density shows that the foam has the highly porous structure necessary for use of the construct for cell seeding. It is known that pore size, pore shape and interconnectivity of these pores affect the cell growth. An ideal 3-D cell carrier should be highly porous for the cells to get nutritional elements, remove wastes and also allow sufficient space for proper extracellular matrix (ECM) formation (Kim and Mooney, 1998).

##### 3.1.2. Foam and Film Thickness

The average thickness of the films, foams and 3-D constructs (film-foams) were measured by a micrometer (Table 3.1). The 3-D construct consists of a film attached to a foam and the decrease in its thickness with respect to the foam was

caused by the preparation method used. The preparation method involves placement of the foam on the film when the film is being made by solvent evaporation. The solvent in film preparation dissolves some of the foam and as it evaporates it creates a dense barrier separating the foam and film regions of the 3-D construct. This would lead to separation of the two cell types used in vitro.

**Table 3.1.** The average thickness of films, foams and film-foams ( $n = 6$ ).

|                   | Films ( $\mu\text{m}$ ) | Foams (mm)      | 3-D Construct (mm) |
|-------------------|-------------------------|-----------------|--------------------|
| Average Thickness | $40 \pm 2$              | $6.11 \pm 0.08$ | $4.08 \pm 0.08$    |

### 3.1.3. Microscopy Observations

#### 3.1.3.1. SEM

SEM observations give information about the morphology of the carriers.

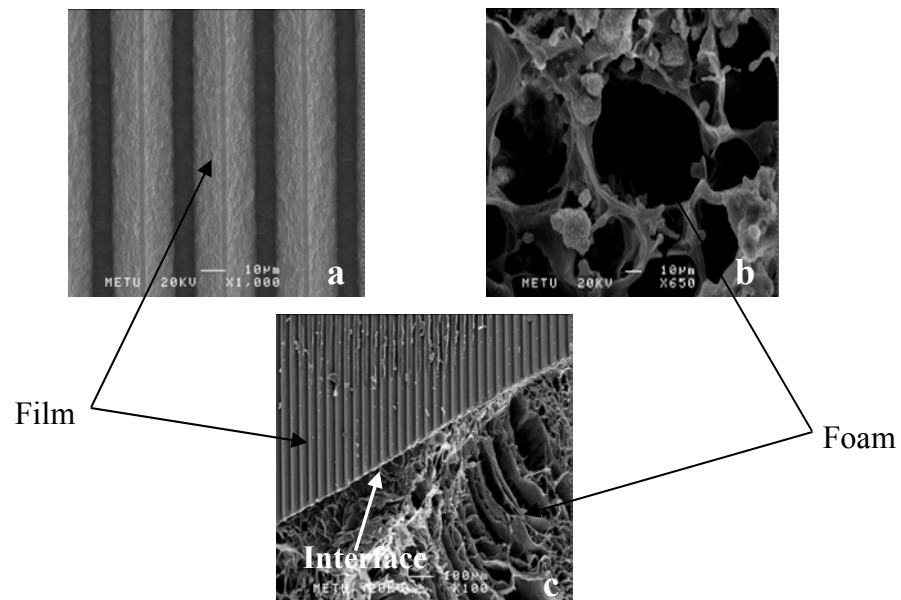


**Figure 3.1.** The SEM micrographs of PLLA-PHBV8 cell carriers. (a) Patterned film, (b) foam and the (c) 3-D construct.

Films prepared on patterned silicon wafers were smooth and the pattern was regular (Fig. 3.1 a). Foams were highly porous as expected from the density calculations (Fig. 3.1 b). The foam and the film of the 3-D construct appeared to be attached tightly to each other with no deterioration of the pattern and the barrier formed at the interface can be seen (Fig. 3.1 c).

### 3.1.3.2. Light Microscopy

Sections (10 and 4  $\mu\text{m}$  thick) of foams were obtained by a microtome and examined under a light microscope to observe the porosity and pore size distribution of the foams. As seen in Figure 3.2, the dark boundaries are the polymer itself. It is evident that the carrier is a highly porous structure suitable for cell seeding. In 4  $\mu\text{m}$  sections, the structure of the pores can be observed better than the 10  $\mu\text{m}$  sections, since in thinner sections the pore overlapping was minimal.

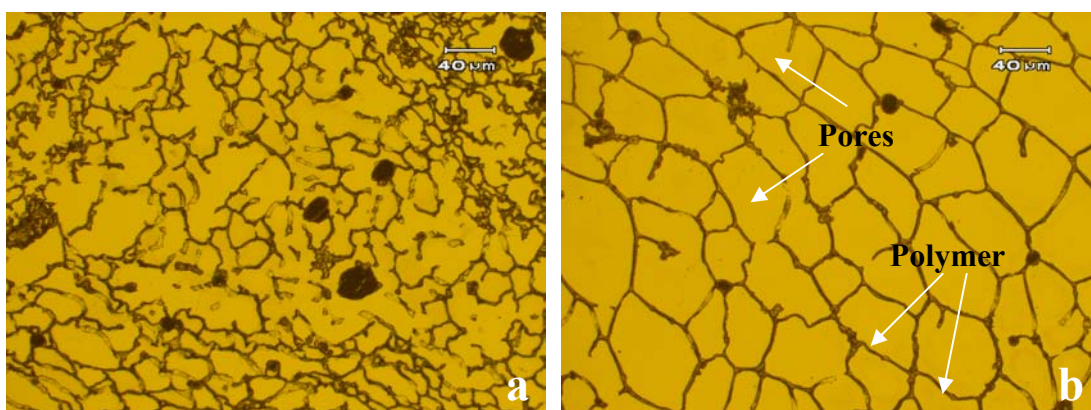


**Figure 3.2.** Light microscopy of foams. Sections were taken by a microtome and the section thickness is 10  $\mu\text{m}$  (a) and 4  $\mu\text{m}$  (b).

### 3.2. In Vitro Studies

In these series three different cell types, Saos-2 cancer cells, D407 RPE cells and 3T3 fibroblasts were tested to study their compatibility with the carriers.

### 3.2.1. Saos-2 Cells on the 3-D Construct

Saos-2 cells were seeded to examine the behavior of cells on the 3-D PLLA-PHBV8 construct with SEM. The micrographs showed that these cells proliferated both on the foam side (Fig. 3.3 a and b) and on the film side (Fig. 3.3 c and d) when seeded exclusively on the film or the foam. On the film side, the cells were located in the grooves but they were not aligned, instead they formed bridges between two ridges (Fig. 3.3 c and d).

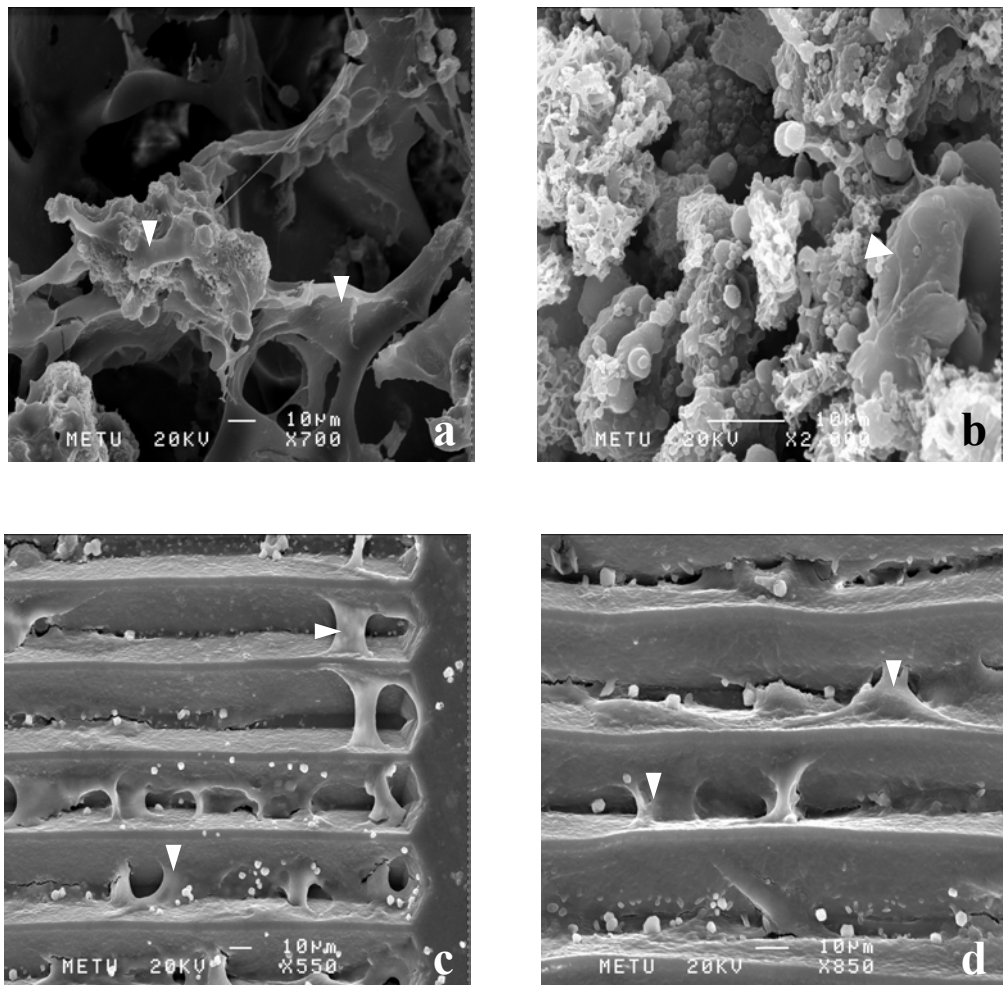


**Figure 3.3.** SEM micrographs of Saos-2 cells on the 3-D construct; (a and b) foam side, (c and d) film side (arrow heads indicate the cells).

### **3.2.2. D407 Cells on Patterned Films**

These RPE cells were tested on the films without any surface treatment or after adsorption of fibronectin on the surface to improve cell adhesion.

#### **3.2.2.1. Without Fibronectin**

##### **3.2.2.1.1. Cell Proliferation**

Cell proliferation was studied by MTS assay as described previously (Section 2.2.3.2.3.1.1.) and a cell number versus OD calibration curve (Appendix A). In this test, 3 films with different patterns and TCPS control were tested. The TCPS control showed an increase in cell number from the beginning, reached a maximum on day 7 before declining due to cell death. The results with all three patterns, there was a lag phase of seven days probably due to the fact that cells could not attach and spread to the polymeric surface as good as on TCPS control (Fig. 3.4) (Steele et al., 1997). At the end of the 14th day, however, the cell number reached the maximum value observed in TCPS before the cells went into a death phase.

The maximum cell number observed on TCPS at 7<sup>th</sup> day was only a 3 fold higher than the day 1 results, while the increase was 19.7 fold in D1 patterned films, 19.5 fold in C3 patterned films and 24 fold in A3 patterned films by day 14. Similar results have been obtained by seeding PLGA films with RPE cells (Lu et al., 2001). Surface of these films were also not modified with any chemical or physical cue and the increase was also 24 fold by day 7.

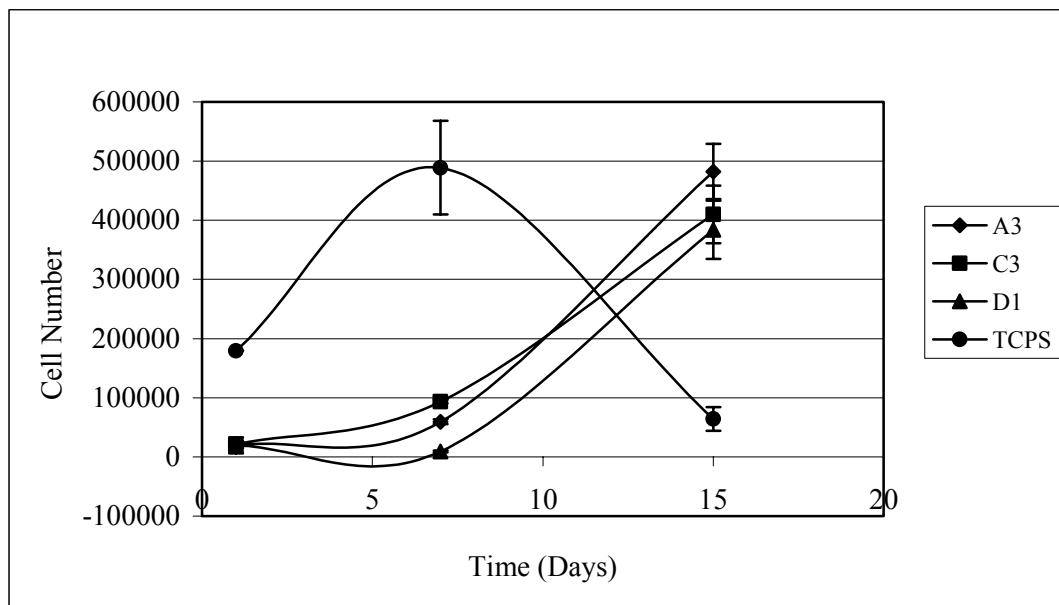


**Figure 3.4.** Growth profile of D407 cells on 3 different micropatterned PLLA-PHBV8 films and TCPS (control) ( $n = 3$ ).

### 3.2.2.1.2. Microscopy Observations

D407 cells were seeded on uncoated, patterned films, and incubated for 14 days at  $37^{\circ}\text{C}$  and 5 %  $\text{CO}_2$  medium. At days 7 and 14, the DNA of the cells were stained with Acridine orange and examined under the fluorescence microscope to observe cell proliferation and distribution. At day 7, D407 cells were low in number and in monolayers (Fig. 3.5 a, c and e). By day 14, they reached confluency and formed multilayers on all three patterns (Fig. 3.5 b, d and f) forming a stratified structure similar to stratified epithelial layer in the cornea. At 14<sup>th</sup> day cell guidance was visible only on A3 films possibly because A3 had the deepest grooves. Although the cells formed 2, or at some places 3, layers cell guidance inside the grooves was still maintained and seen (Fig. 3.5 b). These results are in parallel with the previous studies which has shown that, for both epithelial cells in general (Brunette, 1986) and for corneal epithelial cells in specific (Evans et al., 2005), that grooved surfaces cause contact guidance, and therefore, alignment of the cells along the grooves.

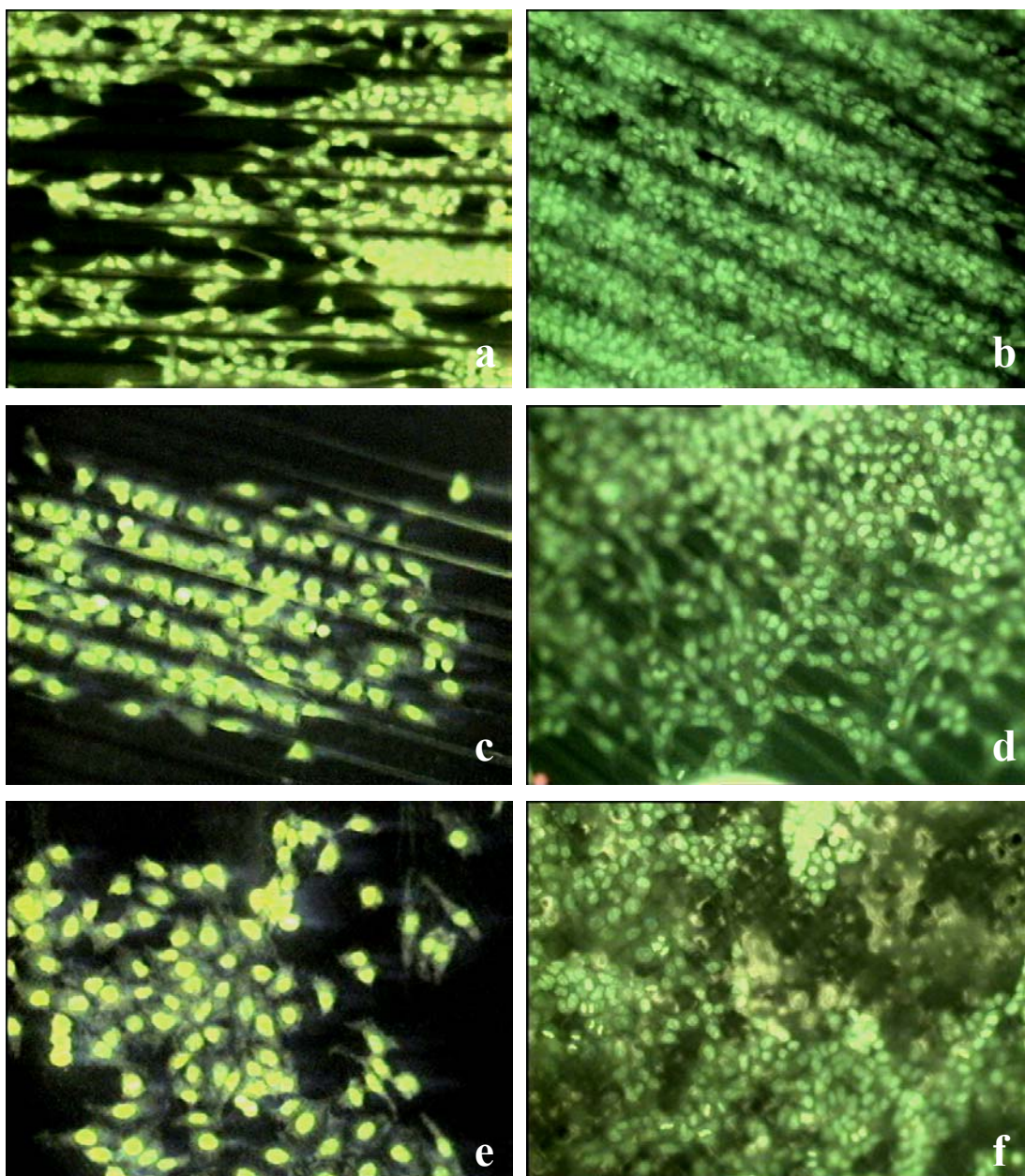


**Figure 3.5.** Fluorescence micrographs of D407 cells seeded on the A3, C3 and D1 patterned films. Observations were made on 7 (a, c, e) and 14 (b, d, f) days (Magnification x10).

### **3.2.2.2. With Fibronectin**

It was earlier reported that surface topography affects corneal epithelial stratification (Dalton et al., 1999). Moreover, stratification was enhanced on topographies with patterns of deeper grooves (Pins et al., 2000). Since the A3 pattern enhanced the stratification of the epithelial cells in its deeper grooves and the increase in cell number was the highest, A3 template was selected for use in the construction of 3-D construct.

It is known that fibronectin takes role in the attachment of corneal epithelial cells. Nishida and his coworkers (1988) showed that fibronectin coating of the culture dishes increased adhesion of corneal epithelial cells in proportion with the fibronectin concentration (Nishida et al., 1988). Therefore, for further studies with A3 patterned films, the surface of the films was coated with fibronectin.

#### **3.2.2.2.1. Cell Proliferation**

Cell proliferation was studied by MTS assays as described previously in Section 2.2.4.1.1. The initial cell attachment, which can be quantified as the number of cells by day 1 with MTS, showed that when fibronectin was adsorbed on the films before seeding, the number of attached cells was much closer to those on TCSP than the uncoated films. There was almost no lag phase in the growth curve of cells seeded on fibronectin coated films possibly for the same reason. Although TCPS reached a higher cell number on day 7, the increase in cell number was only 11 times higher than day 1 whereas it was 60 fold for films. Eventually, they level off and on day 14 the cell numbers were almost the same for both the films and the control (Fig. 3.6).

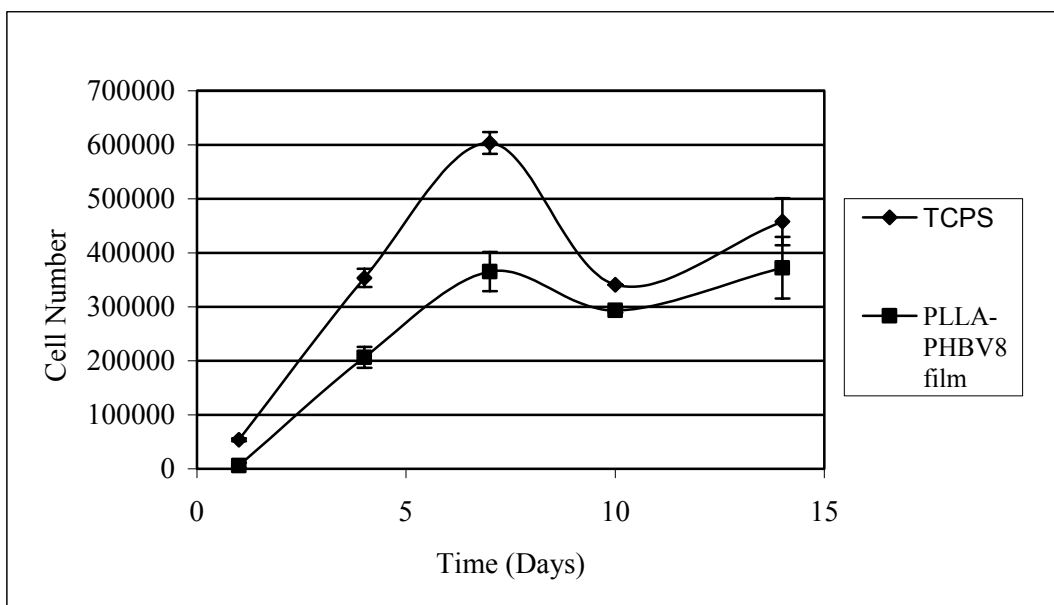


**Figure 3.6.** Growth profile of D407 cells on A3 micropatterned, fibronectin coated PLLA-PHBV8 film and TCPS (control) ( $n = 3$ ).

### 3.2.2.2.2. Microscopy Observations

After seeding the D407 cells on the fibronectin adsorbed films, the films were incubated for 14 days and examined under the fluorescence microscope on days 1, 4, 7, 10 and 14 to observe the proliferation and distribution of the cells.

The result of day 1 is an important parameter which shows the affinity of the cells to a surface (Fig. 3.7). The day 1 micrographs showed that the cells at the seeding site were attached and spread on the surface and guided by the pattern (Fig. 3.7 a and b). However, towards the edges of the film, the cell number decreased and at the edges there were no cells (Fig. 3.7 c and d).

On day 4, the cells had proliferated and they were not localized only at the initial seeding site (Fig. 3.8 a and b) but could be seen at the edges of the film (Fig. 3.8 c and d).

On day 7, cells started to form multilayers at the initial seeding site (Fig. 3.9 a and b), and proliferated at the edges of the film (Fig. 3.9 c and d).

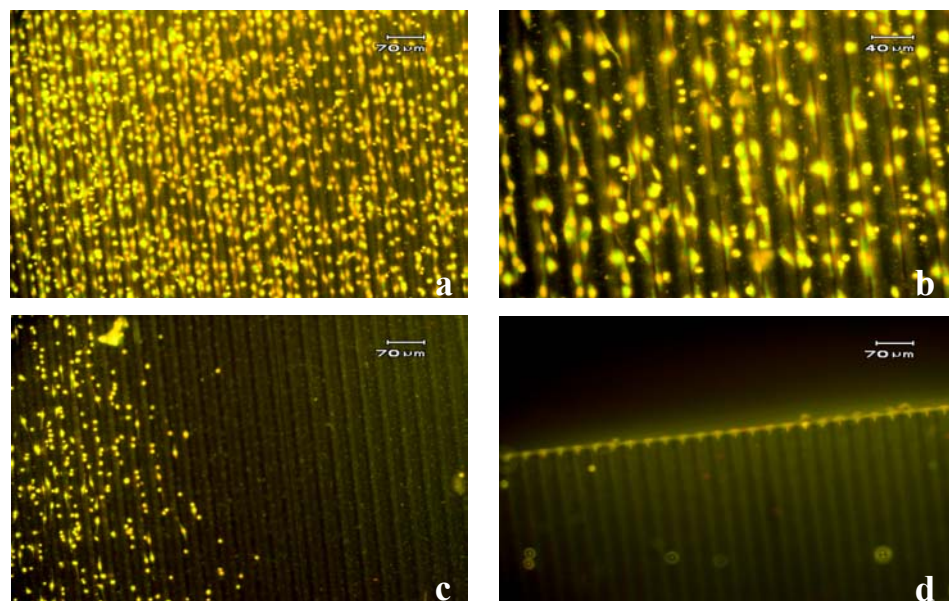


**Figure 3.7.** D407 cells on A3 micropatterned, fibronectin coated films, stained with Acridine orange, on day 1 (a and b are the micrographs of the initial seeding site, c is towards the edge and d is the edge of the film).

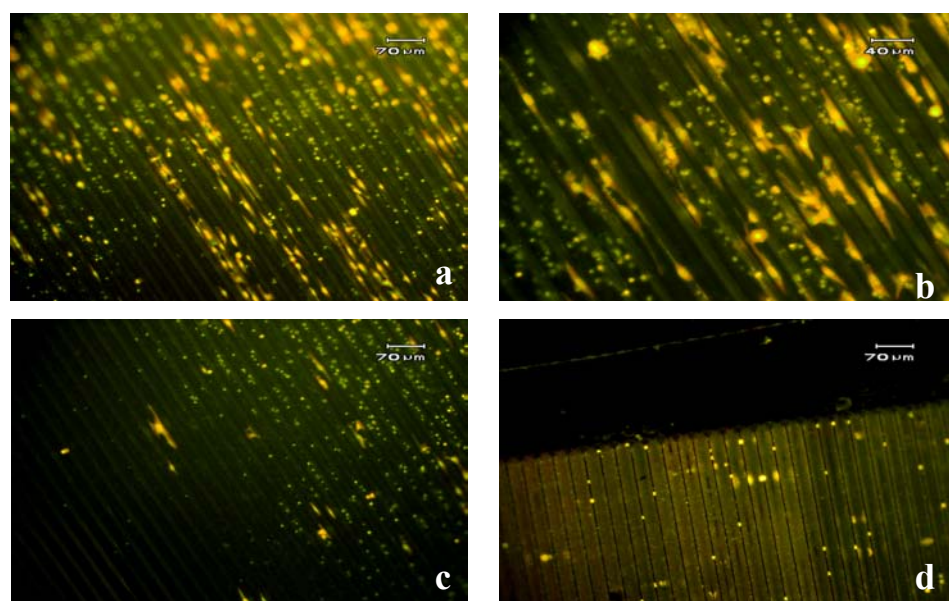


**Figure 3.8.** D407 cells on A3 micropatterned, fibronectin coated films, stained with Acridine orange, on day 4 (a and b are the micrographs of the initial seeding site, c is towards the edge and d is the edge).

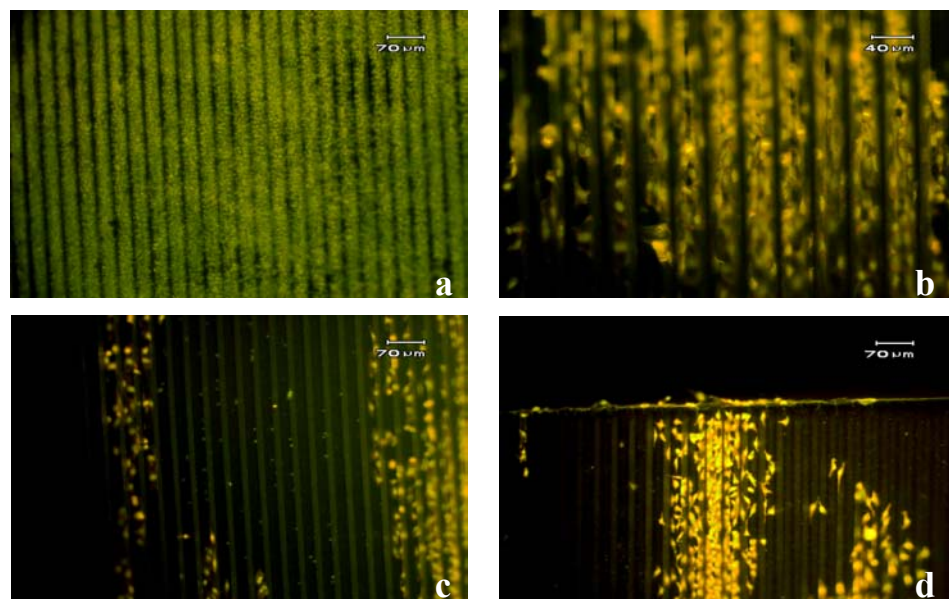


**Figure 3.9.** D407 cells on A3 micropatterned, fibronectin coated films, stained with Acridine orange, on day 7 (a and b are the micrographs of the initial seeding site, c is towards the edge and d is the edge).

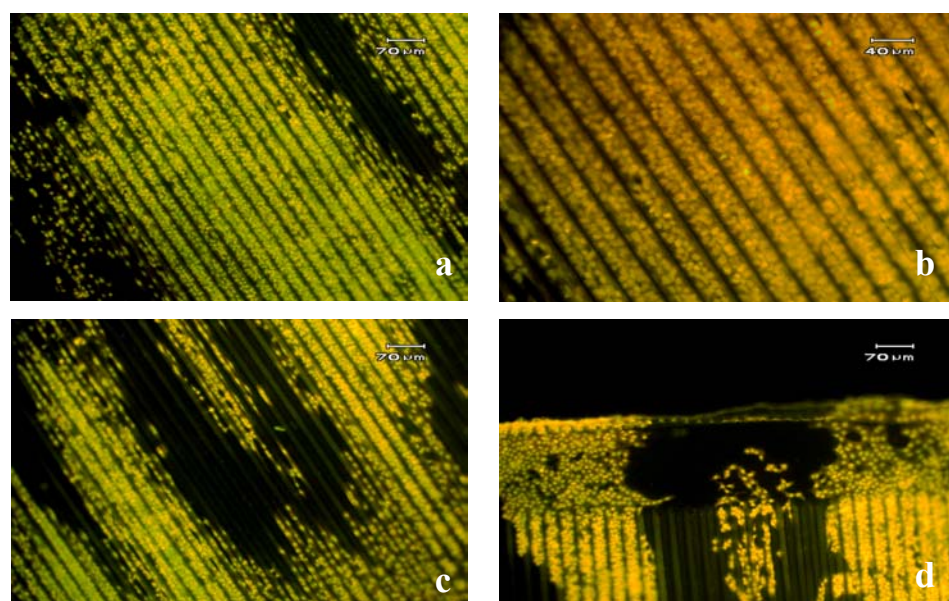


**Figure 3.10.** D407 cells on A3 micropatterned, fibronectin coated films, stained with Acridine orange, on day 10 (a and b are the micrographs of the initial seeding site, c is towards the edge and d is the edge).

On day 10, the cells almost reached confluency on all regions of the film and formed multilayers on most regions (Fig. 3.10).

On day 14, they were confluent on all areas of the film and also formed multilayers on all regions (Fig. 3.11).

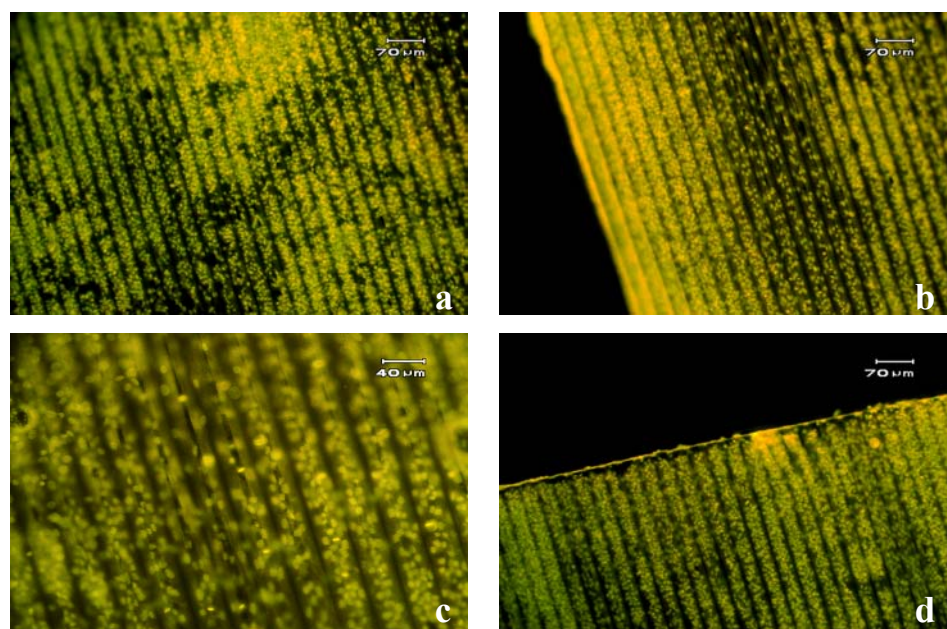


**Figure 3.11.** D407 cells on A3 micropatterned, fibronectin coated films, stained with Acridine orange, on day 14 (a and b are the micrographs of the initial seeding site, c is towards the edge and d is the edge).

### 3.2.2.2.3. Immunohistochemical Analysis

#### 3.2.2.2.3.1. Anti Pan-Cytokeratin Staining

Cytokeratins are the lineage markers for epithelial cells and therefore, this stain labels specifically the epithelial cells such as D407. Staining was done to show that the cells conserved their epithelial character during the culture period (Fig. 3.12).

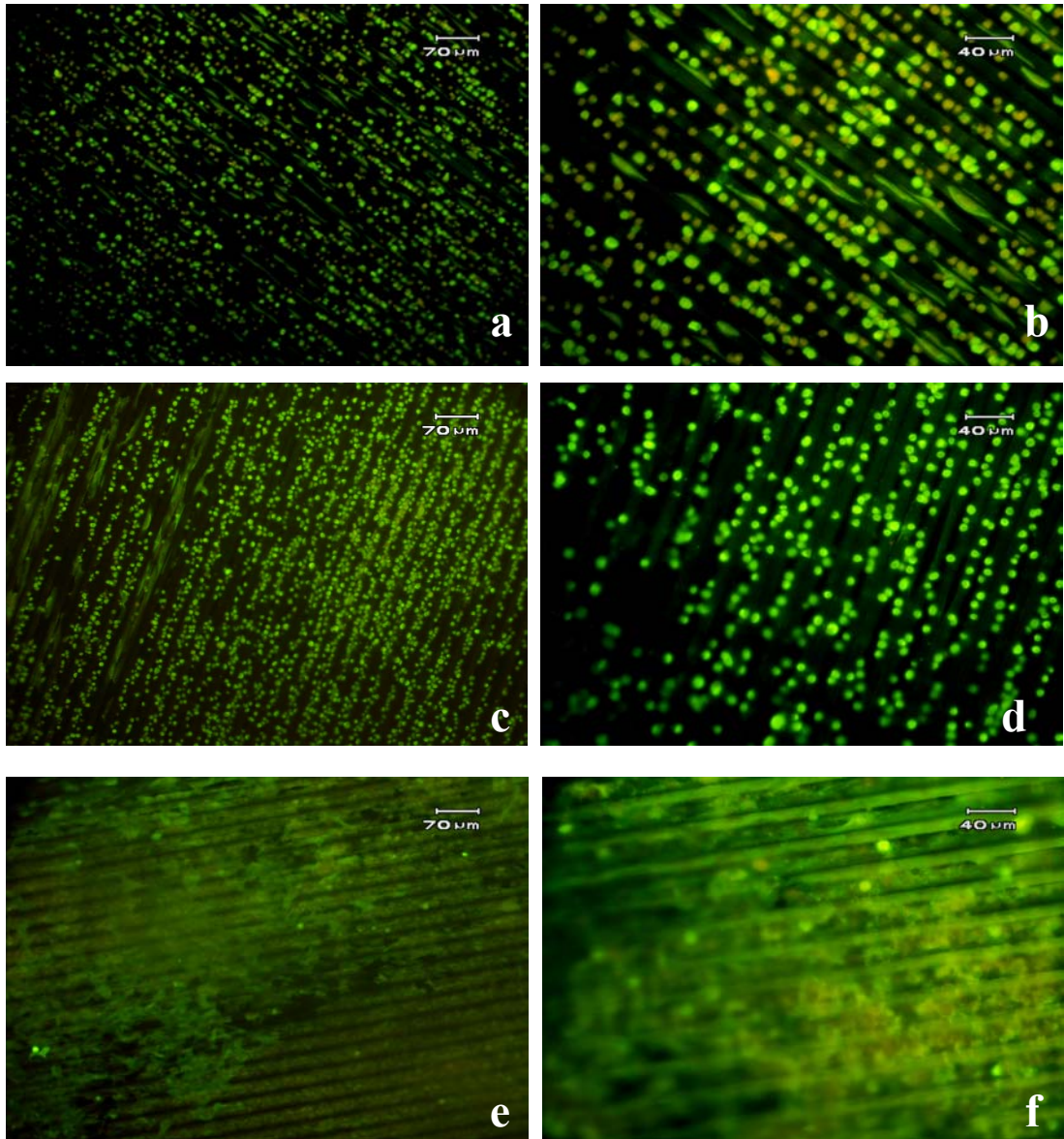


**Figure 3.12.** Anti Pan-Cytokeratin staining of D407 cells on A3 micropatterned, fibronectin coated films on days 1 (a and b), 7 (c and d) and 14 (e and f).

#### 3.2.2.2.3.2. Anti ZO-1 Staining

ZO-1 is a membrane associated protein that is a component of corneal epithelial tight junction complexes. Tight junction formation by epithelial cells is important because the primary function of epithelial cells is to form a barrier or a layer

of protection. In cornea, epithelial layer prevents leakage and regulates passage of molecules in and out of the inner layers of the cornea (Ban et al., 2003). Staining was done to show that D407 cells formed tight junctions, and therefore, the cells were functional (Fig. 3.13).

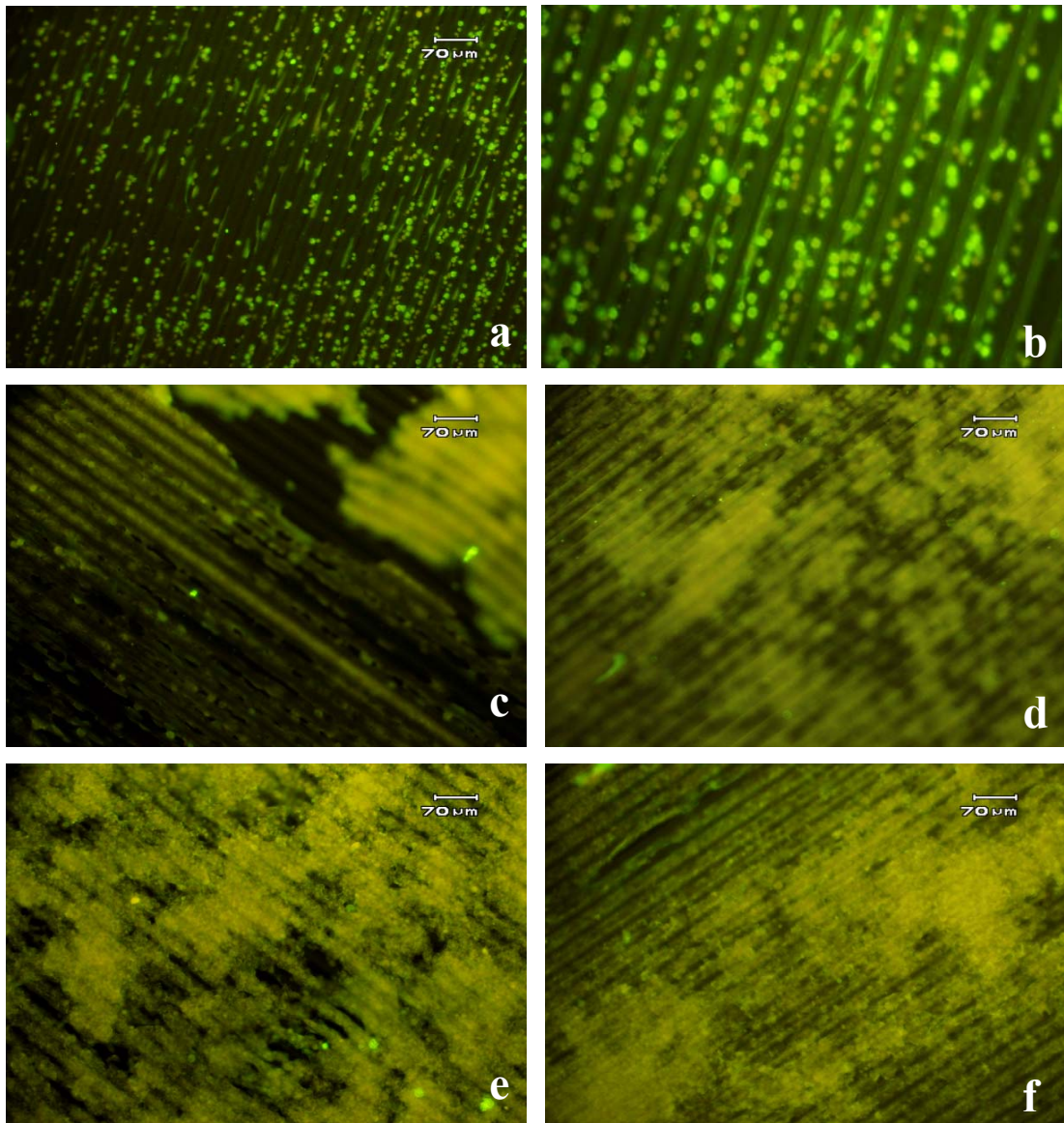


**Figure 3.13.** Anti ZO-1 staining of D407 cells on A3 micropatterned, fibronectin coated films on days 1 (a and b), 7 (c and d) and 14 (e and f).

It is observed that as the time is longer more is functionality of the cells and more of the surface is covered both in 2-D and in 3-D. It can thus be concluded that the D407 cells used have retained their phenotype during these experiments.

### **3.2.3. 3T3 Cells on Foams**

#### **3.2.3.1. Cell Proliferation**

Two different initial cell seeding densities were used to study 3T3 proliferation and distribution within the foams. Cell proliferation was studied by MTS assay as described previously in Section 2.2.4.1.1. and a cell number versus OD calibration curve (Appendix B).

Seeding was done with a density of  $5 \times 10^5$  cells/foam and cell numbers were determined (Fig. 3.14). On TCPS the cell number increased from a value of  $6 \times 10^5$  on day 1 to a maximum of  $10^6$  on day 4, dropped to  $2 \times 10^5$  on day 7 and increased to  $9 \times 10^5$  on day 14. On foams the cell number of  $2.5 \times 10^5$  on day 1 did not change for 3 days and then increased to  $4 \times 10^5$  on day 7, decreased to  $3 \times 10^5$  on day 7 and then started to increase again. These changes were probably because the increased cell number limited the space available and thus became insufficient for survival. They went into a death phase, this increased the space available, and helped the remaining viable cells to increase in number again. The fluctuation in cell number was higher in TCPS since it was a two dimensional carrier and access to nutritional elements was not difficult as a 3-D foam. The maximum cell numbers obtained in foams were  $4.2 \times 10^5 \pm 6 \times 10^4$  and  $4.9 \times 10^5 \pm 7 \times 10^4$  cells on days 7 and 14, respectively. The MTS results showed that initial seeding density of  $5 \times 10^5$  cells/foam was too high because of both the fluctuations and low cell numbers.

The initial seeding density was then decreased to  $2.5 \times 10^5$ . The MTS results showed that the fluctuation was less and the cell number reached was  $5.6 \times 10^5 \pm 2 \times 10^3$  on day 14 (Fig. 3.15). This was higher than the maximum number reached when the initial seeding density was  $5 \times 10^5$  cells/foam (Fig. 3.16). Also, the increase

in cell number by day 14 was significantly higher (3 fold). This is a good result because in a previous study with fibroblasts on 3-D collagen carriers the increase was only 1.5 fold in 21 days and there was fluctuation of cell number on these carriers, too (Besseau et al., 2002). In another study with porous PHBV foams, it was shown that these carriers were more suitable for fibroblast culturing than collagen foams. PHBV foams maintained their integrity in culture conditions and the cells on these foams were twice as functional as the ones on collagen foams as judged the total protein production after 4 weeks of cell culture (Rivard et al., 1995).

From these results, initial seeding density of  $2.5 \times 10^5$  cells/foam was decided to be used on 3-D constructs.

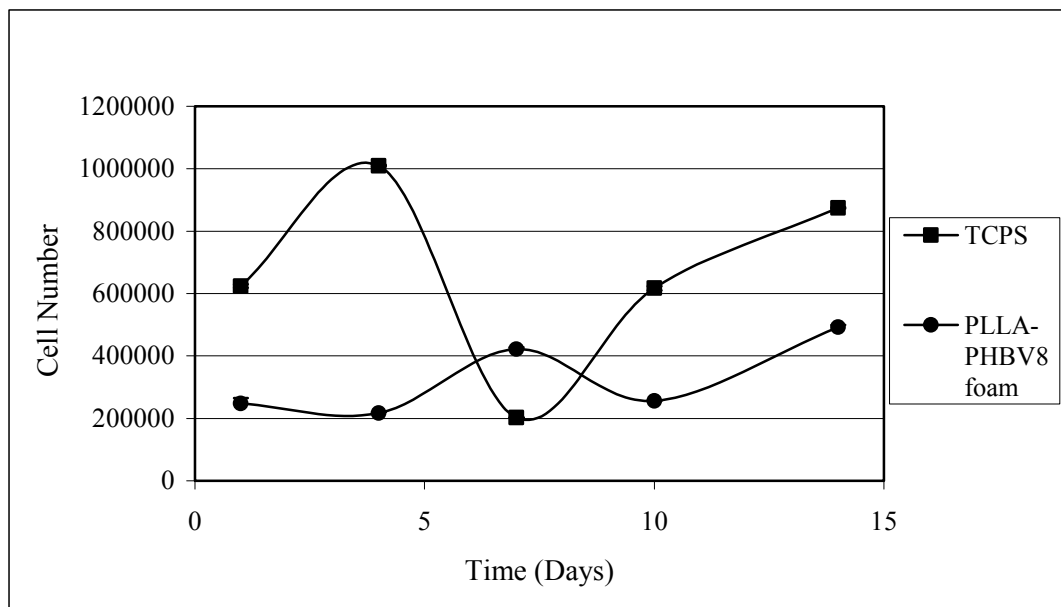


**Figure 3.14.** Growth profile of 3T3 cells (initial seeding density of  $5 \times 10^5$  cells) on foams and TCPS (control) ( $n = 3$ ).

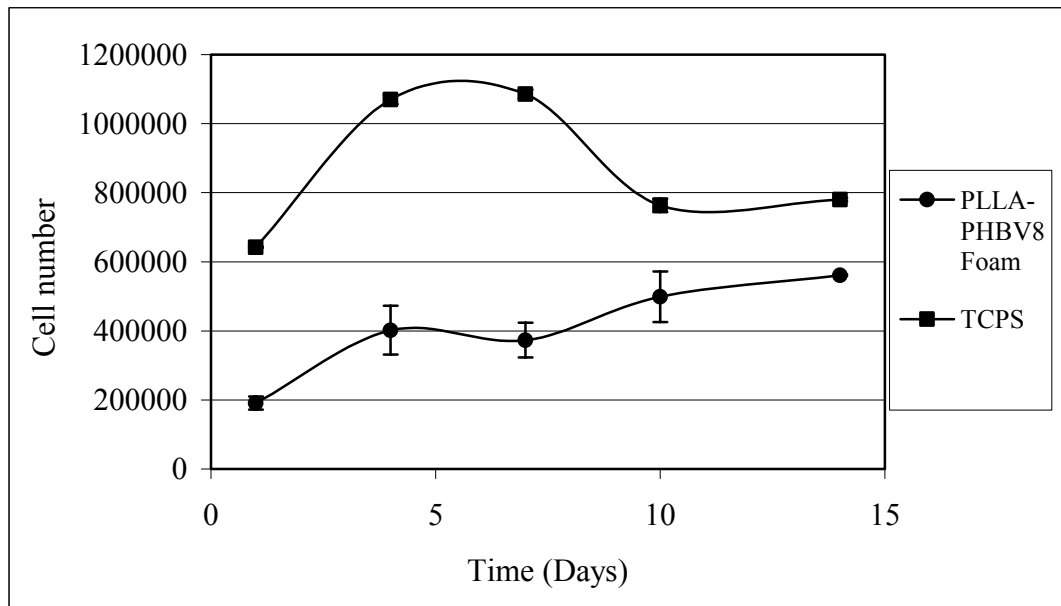


**Figure 3.15.** Growth profile of 3T3 cells (initial seeding density of  $2.5 \times 10^5$  cells) on foams and TCPS (control) ( $n = 3$ ).

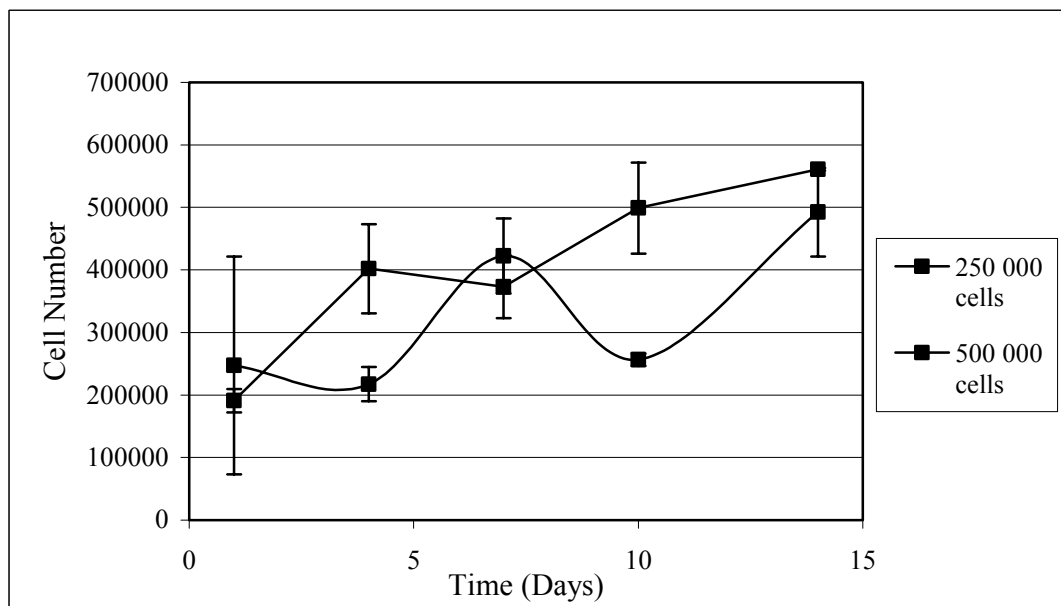


**Figure 3.16.** Growth profile of 3T3 cells with different initial seeding densities ( $2.5 \times 10^5$  and  $5 \times 10^5$ ) on PLLA-PHBV8 foams ( $n = 3$ ).

### 3.2.3.2. Microscopy Observations

#### 3.2.3.2.1. SEM

3T3 seeded ( $2.5 \times 10^5$  cells/foam) PLLA-PHBV8 foams were examined under SEM on days 7 and 14.

On day 7, 3T3 cells on the upper side of the foam, where the seeding was done, were significantly high in number both on the top (Fig. 3.17 a) and in the regions somewhat below it (Fig 3.17 b). However, towards the core of the foam the number of cells that can be seen in the micrographs decreases significantly (Fig 3.17 c). This is probably due to the foam being thick. Since the foams were  $6.11 \pm 0.08$  mm thick and seeding was done from the top of the foams, the distance to be travelled by the cells to reach to the central regions by day 7 was very high. On day 14 however, more cells could be seen in the middle portions of the foam (Fig 3.18 c). The MTS results (Section 3.2.3.1) indicated that there were  $1.9 \times 10^5$  more cells on day 14 than on day 7 ( $5.6 \times 10^5$  and  $3.7 \times 10^5$ , respectively). However, the cells on the micrographs of day 14, were not as distinguishable as the cells on day 7 micrographs, even in the micrographs taken from the top view of the foam where the cells were expected to be located most (Fig. 3.18 a and b). Also, the polymer fibers were not smooth, there seemed to be a deposition on them and the pores were seemed to be blocked with some kind of plaque formation (Fig 3.18). These can be interpreted as the 3T3 cells secreted large amounts of ECM in the regions they reached confluency by day 14. Also, they continued to proliferate within the foam towards the central regions, again by secreting ECM but in lower amounts, therefore, the cells can be distinguished (Fig 3.18 c).

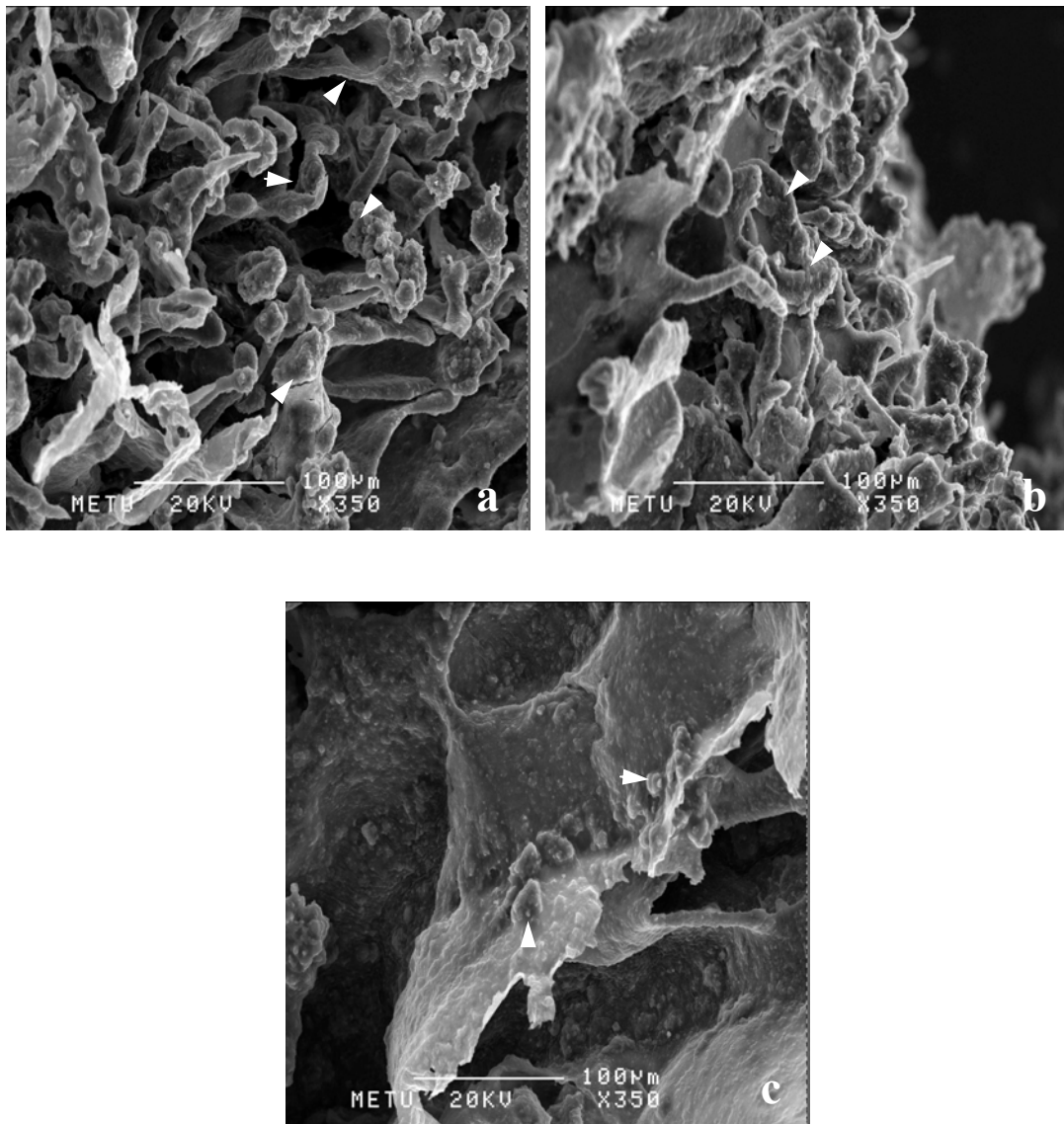


**Figure 3.17.** SEM micrographs of 3T3 seeded PLLA-PHBV8 foams on day 7 (a) is the top view, (b) is the cross-section towards the top and (c) is the cross-section of the middle portion (arrows indicate cells).

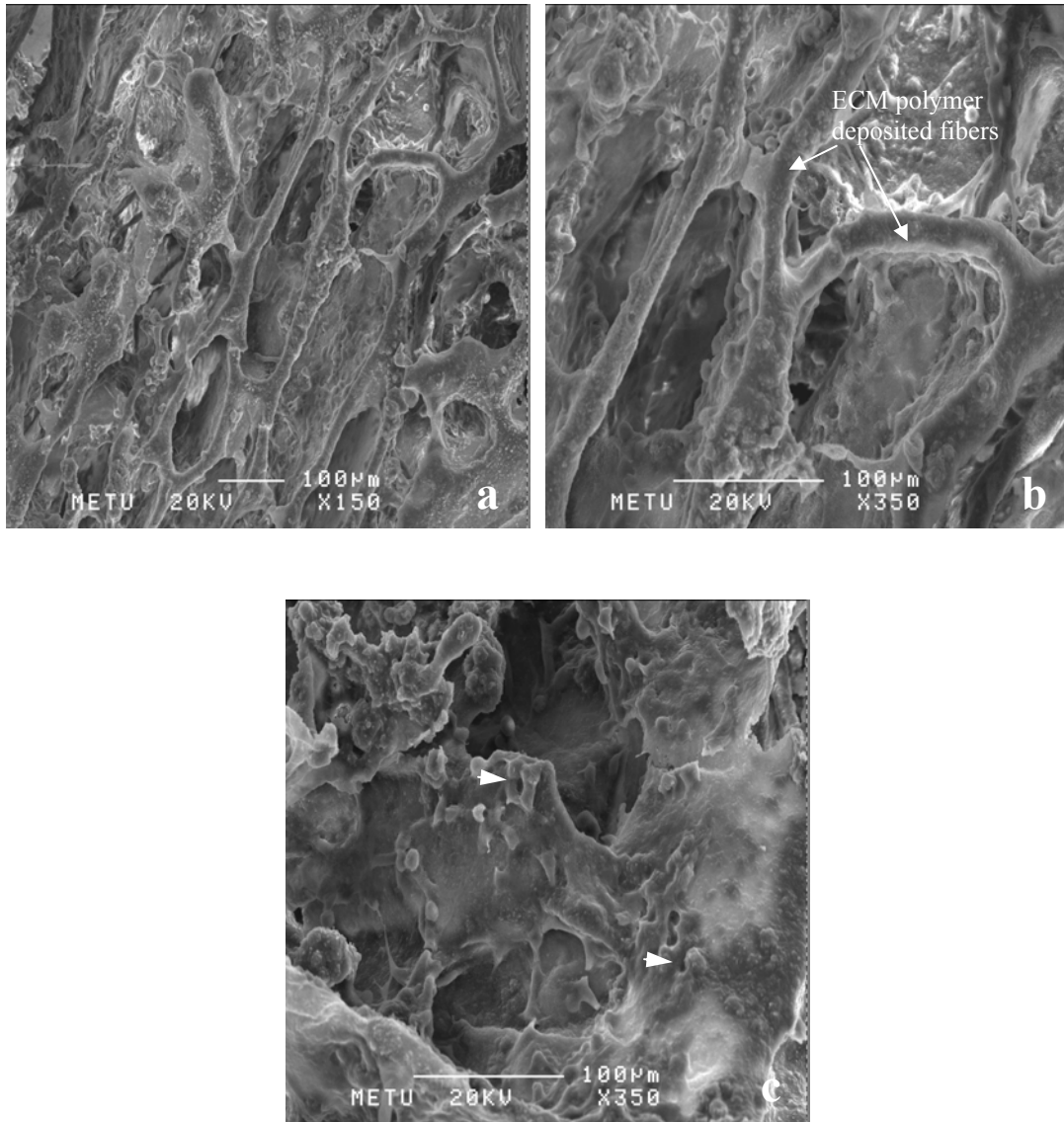


**Figure 3.18.** SEM micrographs of 3T3 seeded PLLA-PHBV8 foams on day 14. (a) and (b) are the top views, (c) is the cross-section of the middle portion (arrow heads indicate cells).

### 3.2.3.2.2. Confocal Microscopy

3T3 seeded ( $2.5 \times 10^5$  cells/foam) PLLA-PHBV8 foams were examined under confocal microscope after staining with Acridine Orange on day 14. Since the foam was too thick, only the top 350 μm section of it was examined. The observations

done by confocal microscopy showed the 3-D distribution of the cells within the foam since the principle in confocal microscopy is taking images not only in the x-y direction but also in the z direction. The micrographs showed that the foam was highly porous and the distribution of the cells within the structure was quite homogeneous (Fig 3.19).

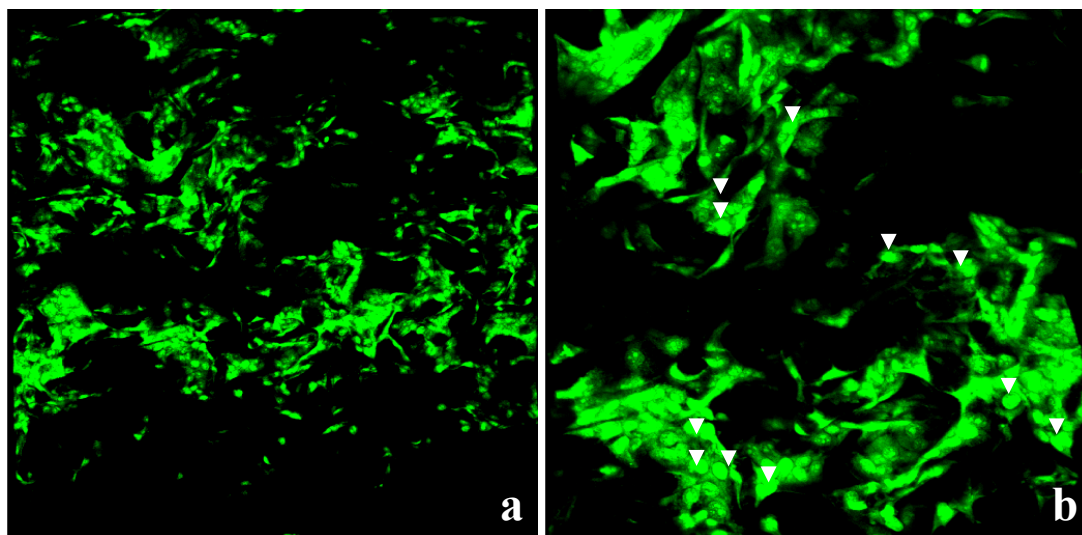


**Figure 3.19.** Confocal microscopy of 3T3 seeded PLLA-PHBV8 foams at day 14. Magnification is 10x for (a) and 20x for (b) (arrow heads indicate cells).

### 3.2.4. D407 and 3T3 Cells on the 3-D Construct

#### 3.2.4.1. Cell Proliferation

Cell proliferation was studied by MTS assay as described previously in Section 2.2.4.1.1. Although the initial cell attachment was lower than the control, the trend was similar. The difference in cell number on the 14<sup>th</sup> day was due to lower initial attachment (Fig. 3.20). Moreover, cell number increase on TCPS at day 7 was only 2 fold whereas it was 9.5 fold for the 3-D construct. The increase in cell number also showed that the 3-D construct was porous enough to allow the cell proliferation.

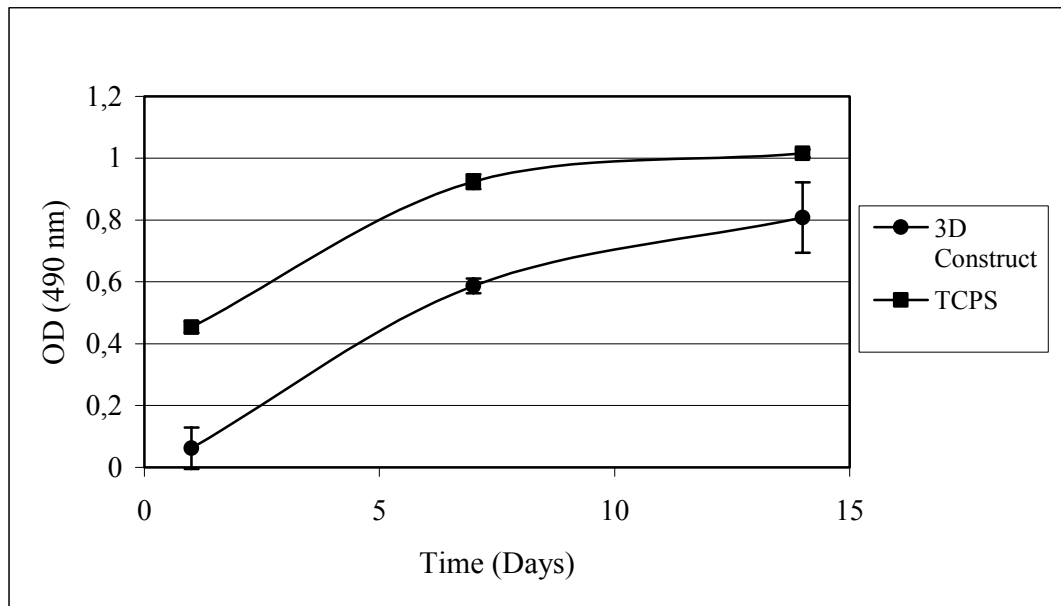


**Figure 3.20.** Growth profile of D407 and 3T3 cells on 3-D construct and TCPS (control) ( $n = 3$ ).

### 3.2.4.2. Microscopy Observations

#### 3.2.4.2.1. Fluorescence microscopy

D407 cells and 3T3 cells were seeded on 3-D construct on film and foam sides, respectively and were incubated for 14 days and examined under the fluorescence microscope on days 7 and 14 to study the proliferation and distribution of the cells. Acridine orange staining was done on vertical sections (showing both the film and the foam, 12  $\mu\text{m}$  in thickness) of the construct by using a microtome.

On day 7, in the central regions of the foams, regions populated with cells (Fig. 3.21 a) and devoid of cells were observed (Fig. 3.21 b).

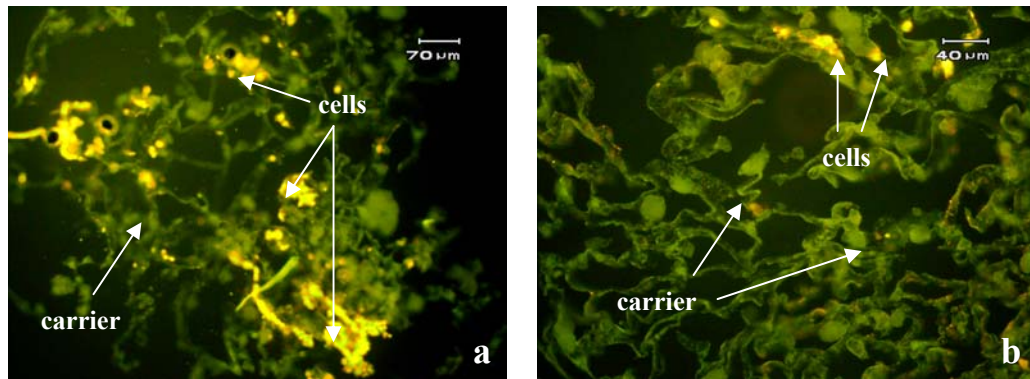


**Figure 3.21.** 3T3 of the 3-D construct (stained with Acridine orange, at day 7).

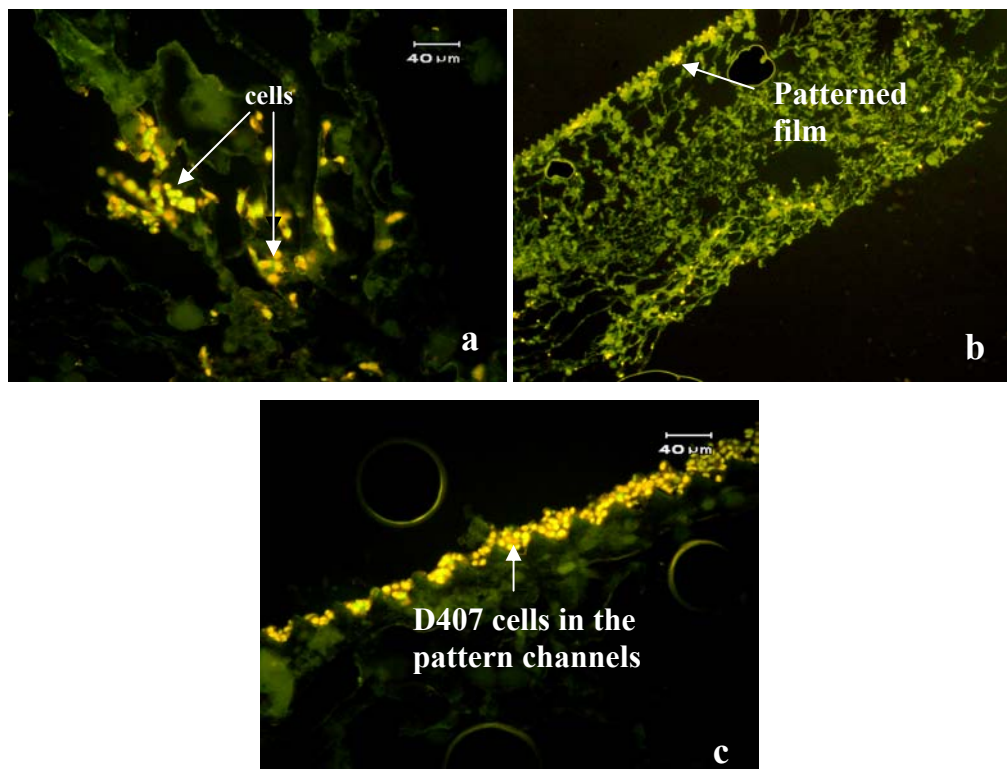


**Figure 3.22.** 3T3 and D407 cells on 3-D construct, stained with Acridine orange, on day 14. The central regions of the foam (a), the general cross-sectional view of the 3-D construct (b), the close-up of the film-foam interface (c).

On day 14, more cells could be seen within the construct (Fig. 3.22 a and b). Also the D407 cell seeded on the film sides of the 3-D construct had formed multilayers as expected from the previous experiments with D407 cells seeded on only micropatterned films (Fig. 3.22 c).

#### **3.2.4.2.2. SEM**

D407 and 3T3 seeded PLLA-PHBV8 3-D constructs were examined with SEM on days 7 and 14.

On day 7, D407 cells on the film side of the construct had proliferated (Fig. 3.23 a) and formed multilayers as could be deduced from the continuous sheets formed by the cells at some regions (Fig. 3.23 b). There were 3T3 cells on the foam, as seen from the bottom (Fig. 3.23 c) and also from the cross-section (Fig. 3.23 d) but not at the level of D407 on the film side.

On day 14, the multilayer formation by D407 cells were more extensive and all the D407 cells became a continuous sheet (Fig. 3.24 a). When the magnification was increased, cells could be seen (Fig. 3.24 b). As seen in Figure 3.24 c, the foam side of the 3-D construct had a regular pore shape and distribution. Also, the pores were interconnected which is a vital property for the seeded cells to survive. Since the seeding was done from the opposite side of the construct and the cells could not proliferate significantly, the area just beneath the film had a few cells even on day 14 (Fig 3.24 d). However, the central regions of the foam contained a large number of cells as well as some deposition on the polymer fibers which could be interpreted as ECM formation (Fig 3.24 e and f).

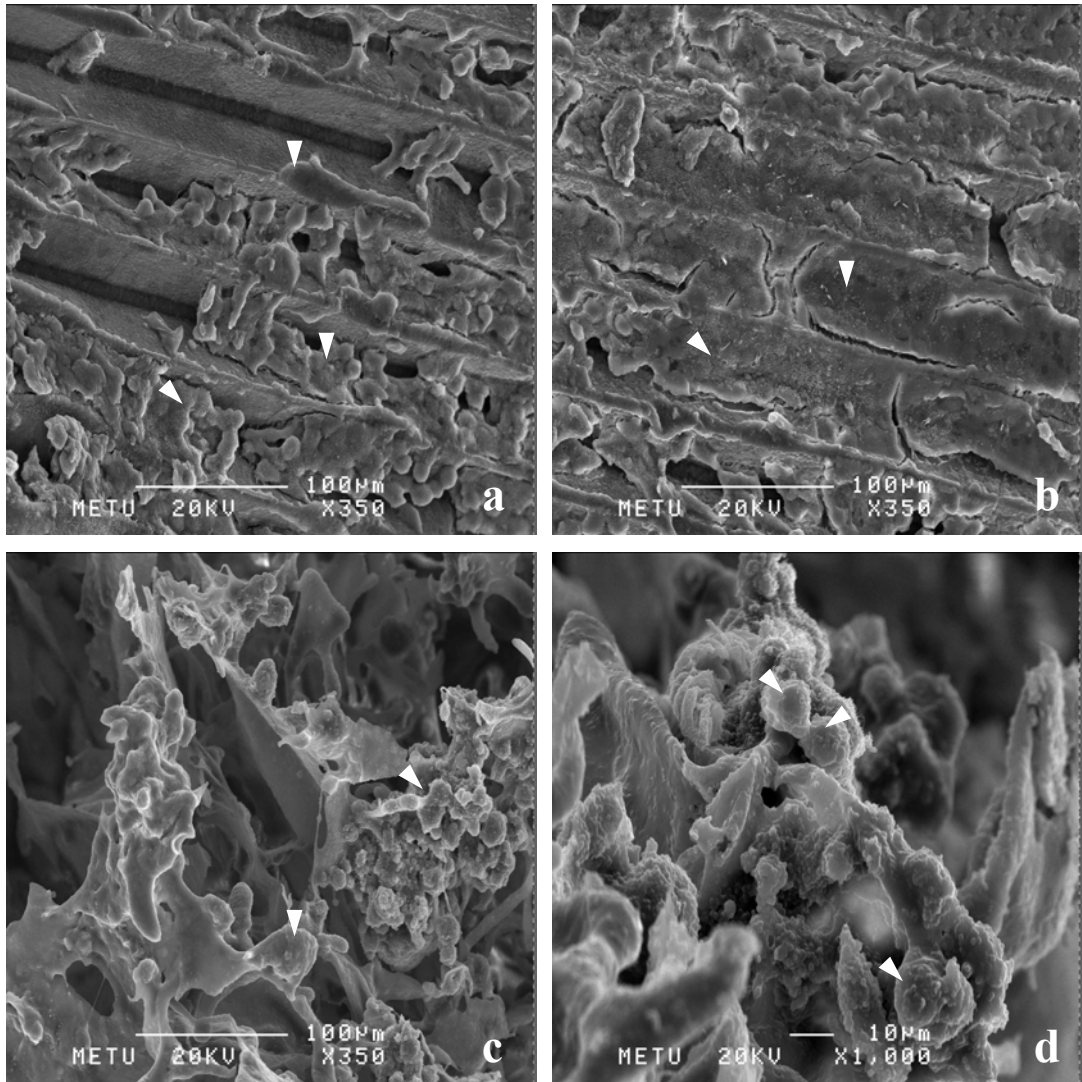


**Figure 3.23.** SEM micrographs of 3-D construct on day 7. (a) and (b) shows the film from the top, (c) is the foam viewed from the bottom and (d) is the cross-section (arrow heads indicate cells).

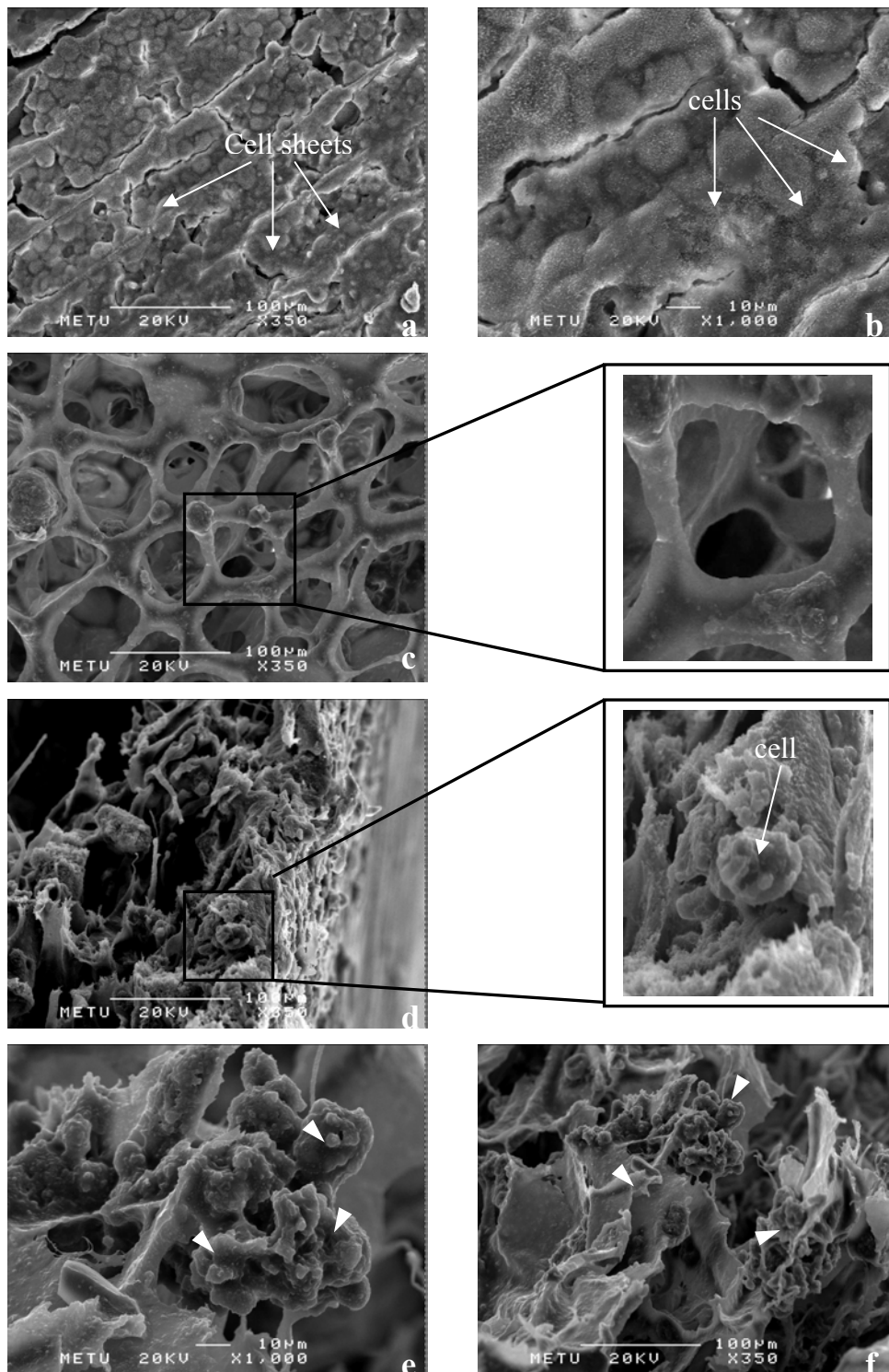


**Figure 3.24.** SEM micrographs of 3-D construct at day 14. (a) and (b) are the film side, (c) is the foam side, (d) is the cross-section view of the foam just under the film, (e) and (f) are the cross-section view of the middle portion of the foam.

### 3.2.4.3. Immunohistochemical Analysis

#### 3.2.4.3.1. Anti Collagen Type-1 Staining

Staining for collagen type I was done to examine the matrix production by 3T3 cells of 3-D construct after 7 and 14 days of incubation.

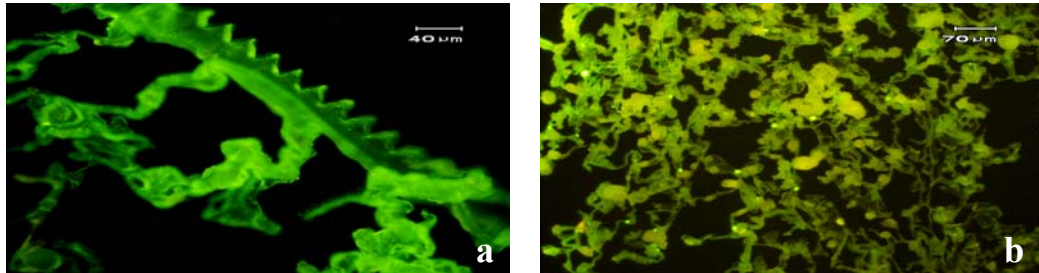


**Figure 3.25.** Anti collagen type I staining of 3T3 cells on 3-D construct at day 7.

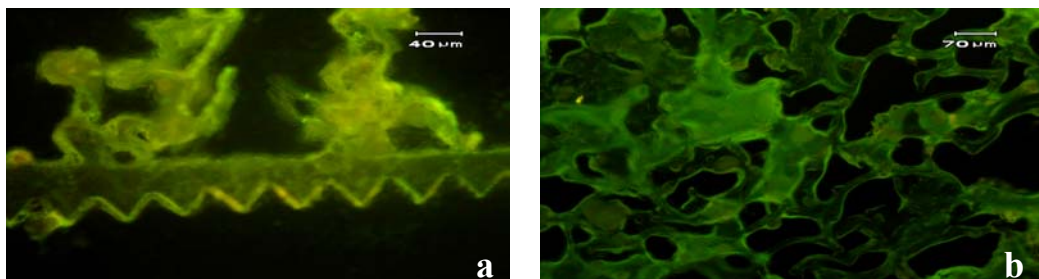


**Figure 3.26.** Anti collagen type I staining of 3T3 cells on 3-D construct at day 14.

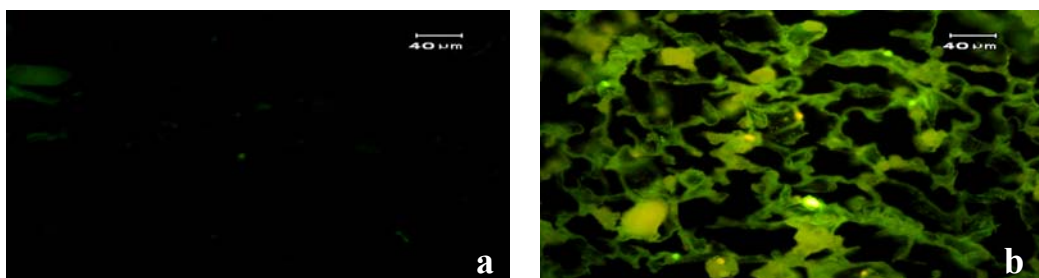


**Figure 3.27.** Comparison of (a) unseeded and (b) seeded, therefore, collagen deposited foam.

The deposition of collagen on the polymer fibers of the 3-D construct could clearly be seen in Figure 3.25 for day 7 and in Figure 3.26 for day 14. To show that the staining was specific for collagen, an empty foam was stained with the same procedure and examined under fluorescence microscope. As seen on Figure 3.27, the staining was specific for collagen.

## CHAPTER 4

### CONCLUSION

End stage organ or tissue failure is a common problem in today's world because of prolonged lifetime of mankind and severe diseases or injuries. In most cases, transplantation from a donor or utilization of mechanical devices are performed to restore function of failed organ. In some cases, use of biomaterials is a good approach to help healing of damaged tissue or maintain its functionality. Because of the drawbacks of these treatments, a new expansion of the biomaterials field, called tissue engineering, has started coming into use for such cases. Tissue engineering aims to reconstruct the failed organs with the use of biodegradable carriers containing cells.

In this study, biodegradable and biocompatible polyester carriers of PLLA-PHBV8 were tested for the tissue engineering of the cornea. D407 and 3T3 cells were seeded on the carriers as model cells for epithelia and keratocytes of the cornea, respectively, and cultured for 14 days. Characterization of these cells and the carriers was done with various microscopic techniques at predetermined time points. The cell number on the carriers was quantified by MTS assay and the functionality of the cells was assessed by immunohistochemistry. Although the polymers themselves were not ideal substrates for the cell attachment, coating of the surface with fibronectin resulted in a higher cell adhesion, close to that of control TCPS. The MTS results showed that cells seeded on the polymeric carriers proliferated significantly more than those on the TCPS. The micropatterned surface of the polymeric films allowed formation of D407 cell multilayers. The microscopic

observations on carriers showed that the polymeric foams had the required highly porous structure and pore interconnectivity for their utilization as cell carriers. From the micrographs of the 3T3 cells seeded on the foams and the 3-D construct it was seen that the cells were distributed quite uniformly in the foam around the initial seeding site. However, the cell number decreased significantly towards the core of the foam, even on day 14 probably because of the high thickness of the foam. To obtain a more homogeneous 3-D construct, the thickness of the foam side needs to be decreased. Immunohistochemical analysis proved that the cells seeded on the carriers were functional. It can, therefore, be concluded that the PLLA-PHBV8 carriers could be seriously considered as cell carriers in future studies on corneal tissue engineering.

## REFERENCES

- Ameen D.B., Bishop M.F., McMullen T. A lattice model for computing the transmissivity of the cornea and sclera *Biophys. J.* 1998; 75: 2520-2531
- Aziz M.A., Rahman M.A. Corneal foreign body-an occupational hazard *Mymensingh Med J.* 2004; 13(2): 174-6
- Ban Y., Dota A., Cooper L.J., Fullwood N.J., Nakamura T., Tsuzuki M., Mochida C., Kinoshita S. Tight junction-related protein expression and distribution in human corneal epithelium *Exp Eye Res.* 2003; 76 (6): 663-9
- Beck R.W., Gal R.L., Mannis M.J., Holland E.J., Cavanagh H.D., Foulks G.N., Heck E.L., Lindquist T., Macsai M.S., Smith R.E., Stark W.J., Stulting R.D., Sugar J. Is donor age an important determinant of graft survival? *Cornea* 1999; 18: 503–10
- Besseau L., Coulomb B., Lebreton-Decoster C., Giraud-Guille M.M. Production of ordered collagen matrices for three-dimensional cell culture *Biomaterials* 2002; 23: 27-36
- Brunette D.M. Spreading and orientation of epithelial cells on grooved substrata *Exp Cell Res.* 1986; 167(1): 203-17
- Buma P., Ramrattan N.N., van Tienen T.G., Veth R.P. Tissue engineering of the meniscus *Biomaterials* 2004; 25(9): 1523-32
- Chen G., Ushida T., Tateishi T. Scaffold design for tissue engineering *Macromol. Biosci.* 2002; 2: 67-77

Chirila T.V., Hicks C.R., Dalton P.D., Vijayasekaran S., Lou X., Hong Y., Clayton A.B., Ziegelaar B.W., Fitton J.H., Platten S., Crawford G.J., Constable I.J. Artificial Cornea *Prog. Polym. Sci.* 1998; 23: 447-73

Chirila T.V. An overview of the development of artificial corneas with porous skirts and the use of pHEMA for such an application *Biomaterials* 2001; 22: 3311-7

Cotsarelis G., Cheng S.Z., Dong G., Sun T.T., Lavker R.M. Existence of slow-cycling limbal epithelial basal cells that can be preferentially stimulated to proliferate: implications on epithelial stem cells *Cell* 1989; 57: 201-9

Cursiefen C., Chen L., Dana M.R., Streilein J.W. Corneal lymphangiogenesis: evidence, mechanisms, and implications for corneal transplant immunology *Cornea* 2003; 22(3): 273-81

Dalton B.A., Evans M.D.M., McFarland G.A., Steele J.G. Modulation of corneal epithelial stratification by polymer surface topography *J Biomed Mater Res.* 1999; 45(4): 384-94

Ehlers N. and Hjortdal J. Corneal thickness: measurement and implications *Experimental Eye Research* 2004; 78: 543-48

Engelmann K., Bednarz J, Valtink M. Prospects of endothelial transplantation *Experimental Eye Research* 2004; 78: 573-78

European Eye Bank Directory, 2003

Evans M.D.M., McFarland G.A., Taylor S., Walboomers X.F. The response of healing corneal epithelium to grooved polymer surfaces *Biomaterials* 2005; 26: 1703-11

Fantes F.E., Hanna K.D., Waring G.O., Pouliquen Y., Thompson K.P., Savoldelli M. Wound healing after excimer laser keratomileusis (photorefractive keratectomy) in monkeys *Arch. Ophthalmol.* 1990; 108: 665-675.

Freyman T.M., Yannas I.V., Gibson L.J. Cellular materials as porous scaffolds for tissue engineering *Progress in Material Science* 2001; 46: 273-282

Germain L., Carrier P., Auger F.A., Salesse C., Guerin S.L. Can we produce a human corneal equivalent by tissue engineering? *Progress in retinal and eye research* 2000; 19: 497-527

Griffith M., Osborne R., Munger R., Xiong X., Doillon C.J., Laycock N.L., Hakim M., Song Y., Watsky M.A. Functional human corneal equivalents constructed from cell lines *Science* 1999; 286(5447) :2169-72

Harkness R.D. Biological function of collagen *Biol. Rev.* 1961; 36: 399-463

Hicks C.R., Fitton J.H., Chirila T.V., Crawford G.J., Constable I.J. Keratoprotheses: advancing toward a true artificial cornea *Surv Ophthalmol.* 1997; 42(2): 175-89

Hogan M.J., Alvarado J.A., Weddel, J.E. The cornea *In Histology of the human eye* 1971; 85-111; W.S. Saunders, Co, Philadelphia

Jester J.V., Petroll W.M. Cavanagh H.D. Corneal stromal wound healing in refractive surgery: the role of myofibroblasts *Prog. Ret. Eye Res.* 1999; 18: 311- 356

Kim B.S. and Mooney D.J. Development of biocompatible synthetic extracellular matrices for tissue engineering *TIBTECH* 1998; 16: 224-30

Kivela T. and Uusitalo M. Structure, development and function of cytoskeletal elements in non-neuronal cells of the human eye *Prog. Retin. Eye Res.* 1998; 17: 385-428

Kruse F.E. Stem cells and corneal epithelial regeneration *Eye* 1994; 8: 170-183

Langer R. and Vacanti J. P. Tissue engineering *Science* 1993; 260: 920-926

Langer R. Biomaterials in drug delivery and tissue engineering: one laboratory's experience *Acc. Chem. Res.* 2000; 33: 94-101

Latkany R., Tsuk A., Sheu M., Sheu S., Loh I., Loh H., Trinkaus V., Randall V. Plasma surface modification of artificial corneas for optimal endothelialization *J. Biomed. Mater. Res.* 1996; 36: 29-37

Lau C.H., Nicholls S.M., Easty D.L. A murine model of interlamellar corneal transplantation *Br J Ophthalmol* 1998; 82: 294-99

Lee C.H., Singla A., Lee Y. Biomedical applications of collagen *International Journal of Pharmaceutics* 2001; 221: 1-22

Leyh R.G., Wilhelmi M., Rebe P., Fischer S., Kofidis T., Haverich A., Mertsching H. In vivo repopulation of xenogeneic and allogeneic acellular valve matrix conduits in the pulmonary circulation *Ann Thorac Surg.* 2003; 75(5): 1457-63

Li H. and Chang J. In vitro degradation of porous degradable and bioactive PHBV/wollastonite composite scaffolds *Polymer Degradation and Stability* 2005; 87: 301-7

Lindberg K., Brown M.E., Chaves H.V., Kenuon K.R. Rheinwald J.G. In vitro propagation of human ocular surface epithelial cells for transplantation *Invest. Ophthalmol. Vis. Sci.* 1993; 34: 2672-9

Lu L., Nyalakonda K., Kam L., Bizios R., Göpferich A., Mikos A.G. Retinal pigment epithelial cell adhesion on novel micropatterned surfaces fabricated from synthetic biodegradable polymers *Biomaterials* 2001; 22: 291-7

Maurice D.M. The structure and transparency of the cornea *J. Physiol.* 1957; 136: 263-86

Michelacci Y.M. Collagens and proteoglycans of the corneal extracellular matrix *Braz J Med Biol Res.* 2003; 36(8):1037-46

Mimura T., Amano S., Usui T., Araie M., Ono K., Akihiro H., Yokoo S., Yamagami S. Transplantation of corneas reconstructed with cultured adult human corneal endothelial cells in nude rats *Exp Eye Res.* 2004; 79(2): 231-7

Minami Y., Sugihara H., Oono S. Reconstruction of cornea in three-dimensional collagen gel matrix culture *Invest. Ophthalmol. Vis. Sci.* 1993; 34: 2315-24

Moller-Pedersen T., Li H., Petroll W.M., Cavanagh H.D., Jester J.V. Confocal microscopic characterization of wound repair after photorefractive keratectomy *Invest. Ophthalmol. Vis. Sci.* 1998; 39: 487-501

Moticka E.J. and She S.C. Comparison of failure rates of orthotopic corneal grafts using three different grafting procedures *Curr. Eye. Res.* 1989; 8: 813-820

Müller L.J., Pels E., Schurmans L.R.H.M., Vrensen G.F.J.M. A new three dimensional model of the organization of proteoglycans and collagen fibrils in human corneal stroma *Exp. Eye Res.* 2004; 78: 493-501

National Eye Institute, 2004

Neuenschwander S. and Hoerstrup S.P. Heart valve tissue engineering *Transplant Immunology* 2004; 12: 359-65

Niemeyer P., Seckinger A., Simank H.G., Kasten P., Sudkamp N., Krause U. Allogenic transplantation of human mesenchymal stem cells for tissue engineering purposes: an in vitro study *Orthopade.* 2004; 33(12):1346-53

Nishida T., Nakagawa S., Watanabe K., Yamada K.M., Otori T., Berman M.B. A peptide from fibronectin cell-binding domain inhibits attachment of epithelial cells *Invest Ophthalmol Vis Sci.* 1988; 29(12): 1820-5

Nishida K. Tissue engineering of the cornea *Cornea* 2003; 22: 28-34

Nishida K., Yamato M., Hayashida Y., Watanabe K., Yamamoto K., Adachi E., Nagai S., Kikuchi A., Maeda N., Watanabe H., Okano T., Tano Y. Corneal reconstruction with tissue-engineered cell sheets composed of autologous oral mucosal epithelium *N Engl J Med.* 2004; 351(12): 1187-96

Pins G.D., Toner M. and Morgan J.D. Microfabrication of an analog of the basal lamina: biocompatible membranes with complex topographies *The FABES Journal* 2000; 14: 593-602

Quirk R.A., France R.M., Shakesheff K.M., Howdle S.M. Supercritical fluid technologies and tissue engineering scaffolds *Current Opinion in Solid State and Materials Science* 2004; In Press, Corrected Proof

Reim M., Kottke A., Schrage, N. The cornea surface and wound healing *Prog. Ret. Eye Res.* 1997; 16: 183-225

Remeijer L., Osterhaus A., Verjans G. Human herpes simplex virus keratitis: the pathogenesis revisited *Ocul Immunol Inflamm.* 2004; 12(4): 255-85

Rivard C.H., Chaput C.J., DesRosiers E.A., Yahia L.H., Selmani A. Fibroblast seeding and culture in biodegradable porous substrates *J Appl Biomater.* 1995; 6(1): 65-8

Schmalenberg K.E., Buettner H.M., Uhrich K.E. Microcontact printing of proteins on oxygen plasma-activated poly(methyl methacrylate) *Biomaterials* 2004; 25: 1851-57

Schrage N.F., Langefeld S., Zschocke J., Kuckelkorn R., Redbrake C., Reim M. Eye burns: an emergency and continuing problem *Burns* 2000; 26: 689-99

Shimmura S. Component surgery of the cornea *Cornea* 2004; 23: 31-5

Steele J.G., Johnson G., Griesser H.J. and Underwood P.A. Mechanism of initial attachment of corneal epithelial cells to polymeric surfaces *Biomaterials* 1997; 18: 1541-1551

Sun J.S., Wu S.Y.H., Lin F.H. The role of muscle-derived stem cells in bone tissue engineering *Biomaterials* 2005; 26: 3953-60

Teebken O.E., Bader A., Steinhoff G., Haverich A. Tissue engineering of vascular grafts: human cell seeding of decellularised porcine matrix *Eur J Vasc Endovasc Surg.* 2000; 19(4): 381-6

Tezcaner A., Bugra K., Hasırcı V. Retinal pigment epithelium cell culture on surface modified poly(hydroxybutyrate-co-hydroxyvalerate) thin films *Biomaterials* 2003; 24: 4573-83

Thoft R.A. and Friend J. The X, Y, Z hypothesis of corneal epithelial maintenance *Invest. Ophthalmol. Vis. Sci.* 1983; 24: 1442-3

Torun Köse G., Korkusuz F., Korkusuz P., Purali N., Özkul A., Hasırcı V. Bone generation on PHBV matrices: an in vitro study *Biomaterials* 2003; 24: 4999-5007

Torun Köse G., Kenar H., Hasırcı N., Hasırcı V. Macroporous poly(3-hydroxybutyrate-co-3-hydroxyvalerate) matrices for bone tissue engineering *Biomaterials* 2003; 24: 1949-1958

Tsai R.J.F. and Tseng S.C.G. Human allograft limbal transplantation for corneal surface reconstruction *Cornea* 1994; 13: 389-400

Tsai R.J.F., Ho Y.S., Chen J.K. The effects of fibroblasts on the growth and differentiation of human bulbar conjunctival epithelial cells in an in vitro conjunctival equivalent *Invest. Ophthalmol. Vis. Sci.* 1994; 35: 2865-75

Vleggeert-Lankamp C.L., Pego A.P, Lakke E.A., Deenen M., Marani E., Thomeer R.T. Adhesion and proliferation of human Schwann cells on adhesive coatings *Biomaterials* 2004; 25(14): 2741-51

Walboomers X.F. and Jansen J.A. Cell and tissue behavior on micro-grooved surfaces *Odontology* 2001; 89: 2-11

Walochnik J., Duchene M., Eibl H., Aspöck H. Treatment of Acanthamoeba keratitis: possibilities, problems, and new approaches *Wien Klin Wochenschr.* 2003; 3:10-7

Williams S.F., Martin D.P., Horowitz D.M. and Peoples O.P. PHA applications: addressing the price performance issue: I. Tissue engineering *International Journal of Biological Macromolecules* 1999; 25: 111-21

Zieske J.D., Mason V.S., Wasson M.E., Meunier S.F., Nolte C.J.M., Fukai N., Olsen B.R., Parenteau N.L. Basement membrane assembly and differentiation of cultured corneal cells: importance of culture environment and endothelial cell interaction *Exp. Cell Res.* 1994; 214: 621-33

## APPENDIX A

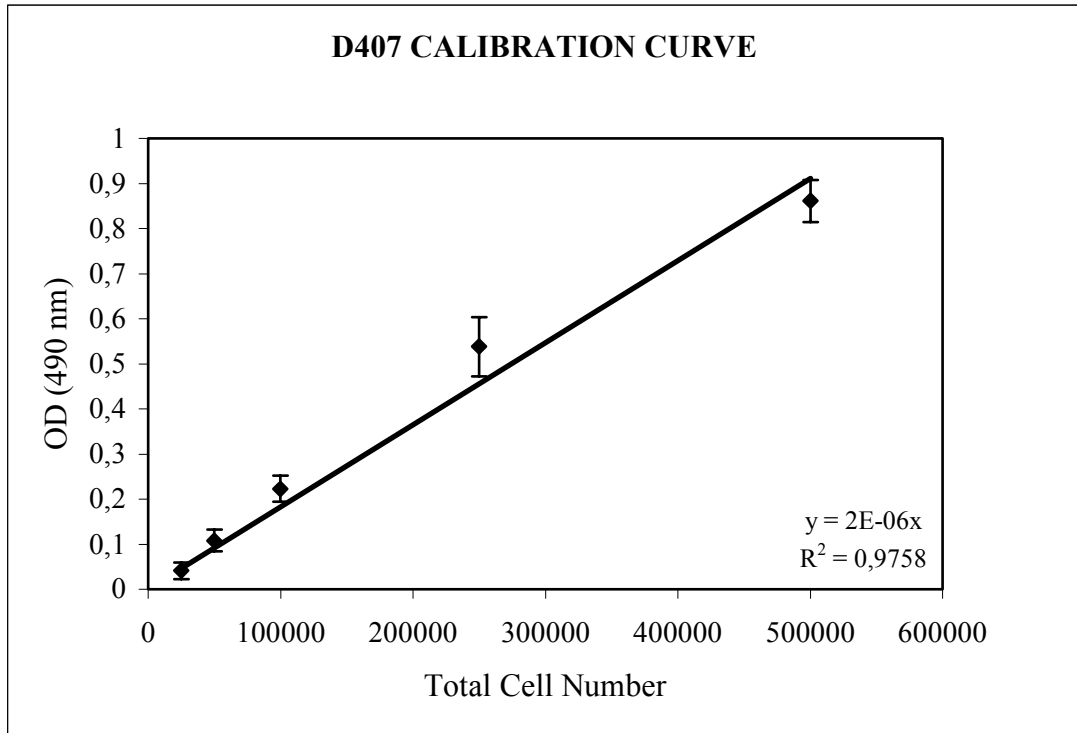


**Figure A.1.** D407 calibration curve obtained by MTS assay.

## APPENDIX B

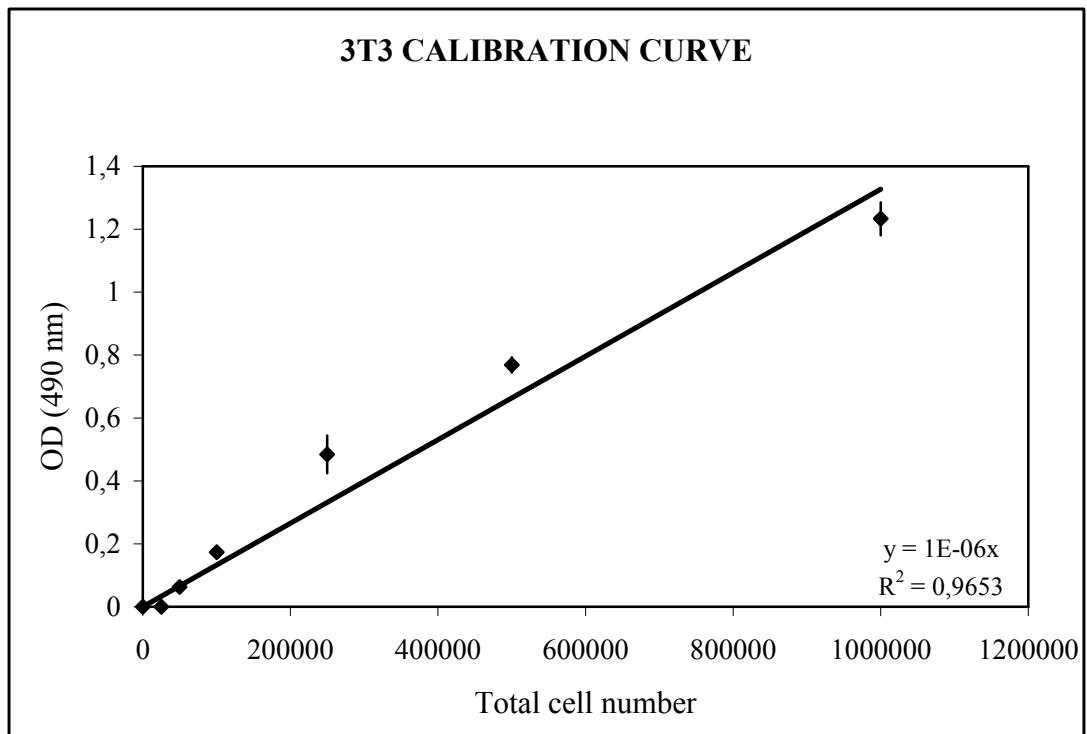


**Figure B.1.** 3T3 calibration curve obtained by MTS assay.